Quantum Double-field Model and Application

Philip B. Alipour*, T. Aaron Gulliver

Department of Electrical and Computer Engineering, University of Victoria, P.O. Box 1700 STN CSC Victoria BC, V8W 2Y2, Canada

ARTICLE INFO

Keywords:
Four measurement variables
Transition probability
State projection
Quantum double-field
Quantum circuit
Pairwise interaction

ABSTRACT

A universal quantum double-field (QDF) model is introduced to predict particle states by doubling their probability outcome. These states are $i = 0$ as ground state (GS), 1 as excited state (ES), $|2\rangle$ as 0 and 1 denoting quantum superposition. A GS particle (Bob) interacts with particles over distance d to attain a target state (TS) with mode m as $|i_m\rangle$ e.g., a particle obeying Bose-Einstein condensate (BEC) or Fermi-Dirac statistics. A scalar κ is used to identify the *effect* caused by light-matter interactions based on its value under a QDF transformation. A transition density matrix via κ provides state transition probabilities between the GS and ES particle fields. The information on the magnitude of the quantum particle position $|\mathfrak{r}|$ between three traps is gathered by a superposing particle, Alice or Eve, on a spatial magnitude of $|\kappa^2|\varrho \leq 2$, where ϱ is the probability density function for a given state $|2\rangle$. This state is projected by Alice or Eve onto the quantum particle field interacting with Bob's field forming a QDF. The QDF information shared with Bob in a QDF circuit, doubles in probability to occupy space on any scale of $\mathfrak{r}$. If Bob's field entangles with a GS field within the QDF, the TS 1 field is predicted (expected) for Bob to obtain, and vice versa. Here, the κ field probability doubles as the correlation length λ_c between states is measured relative to κ, $\mathfrak{r}$ and d, given the transition density matrix values obtained *prior* to a phase transition. This gives a quantum information transmission via QDF on any scale to simulate BEC, heat engines and quantum communication models. For example, in refrigeration, an efficient cooling of atoms is obtained by sharing the quantum information to reroute atoms that weren't participating in the cooling event to participate.

1. Introduction

In this paper, a quantum double-field (QDF) metric space from a thermodynamic system space S is proposed with N interacting particles. A double-field metric space has been proposed by Refs. [2–4]. Among which, unit ball (Bloch sphere) graphs in Euclidian and Hilbert metric spaces were discussed by [3–5]. The adaptation of such measurement theories determines the probability measure of the connected communication between each pair of particles in the proposed QDF model, such as determining their probability space in doubling, occupation, correlation and information as qubits (a QDF algorithm [5, 7–9]). System S, consists of a classical and a quantum phase transition, CPT and QPT models, respectively, Fig. 1(b). In both models, Alice, Bob, Eve, and $N-3$ particles associated with light-emitting and receiving fields (sensors) *controllably* interact [55], and their interactions are observed over a communication channel, Fig. 1(a). The *interaction controller* is a subsystem of S containing a *channel* and *energy barriers* [7] formed by *traps* (*boxes*) where particles interact and communicate [44, 57]. The particles in communication are *participants* of the communication channel. There are three boxes and a target state (TS) to attain. A TS is *interchangeably* referred to *a prize state to win* by Bob or Alice upon interaction before measurement in any applicable quantum game [14–17]. The system model steps shown in Fig. 1 are:

1. A particle as a game prize to win is in one of the boxes. *In the CPT model, its position as a classical particle is fixed* $\mathfrak{r}$*, until a new cycle of one or more particle-particle interactions initiates. In the QPT model, its position can change with a magnitude of* $|\mathfrak{r}| < \infty$.
2. Alice interacts with the particle, while Bob does not.
3. Bob can interact with one of the boxes.
4. Alice interacts with a box and gives Bob the measurement of a quantum particle in that box (1/3 of the information or a *qubit message*) [18, 55], like a boson.

*Principal corresponding author.
E-mail address: phibal12@uvic.ca (P. B. Alipour)
ORCID(s): 0000-0003-1037-018X (P.B. Alipour)

5. Bob interacts with the trapped quantum particle, and with some probability, switches its position via Alice as a light-matter interaction (as in a QDF circuit [7]) to the other remaining box (a binary choice).
6. $N-1$ particles can interact with Bob to cause a switch in the quantum particle state from a box. Eve, associated with light-emitting and receiving fields, with some probability gathers information by reading the state of each box. Eve, with some probability, shares the information via projection [18, 55] with Bob about the contents of each box. *In the QPT model, as Alice changes the prize position, Eve intercepts any state transfer between boxes based on a quantum state teleportation, e.g., [10, 25–31, 35–37, 44, 57].*
7. Bob can continue interacting with the same box to switch to a TS and win, or remain entangled with the quantum particle as a GS particle.
8. Count Bob's prize wins against Alice's wins in S by an adder Hamiltonian as a set of GSs and ESs [7].

In step 8, Alice's win is a TS attained by Alice as a prize state. In a quantum experiment, this TS is the opposite of Bob's TS, *only if one prize state is attainable* by Bob, Alice or any other particle. If there are many prize states e.g., valuable and less valuable prizes ranging from high to low energy states, Alice and Bob can mutually win, as their TS's fall within the GSs of a QPT. For example, in Fig. 1(b), a GS particle Bob interacts with particles over a distance to attain a TS of mode m (of frequency ω) inside a box as a Bose-Einstein condensate (BEC), where $m \in [1, \infty]$. Alice, with the assumption of being a *photonic probe* observing Bob in Fig. 1, can attain the same TS via photonic projections for Bob or other particles. Here, their TS's are degenerate giving the same value of energy upon measurement, Sec. 2. Examples of experimental events and outcomes can be simulated in a QDF game model as shown in Appx. A. The physical method to examine the QDF system model and its adaptation to a QDF game is presented in [7]. The model steps can be evaluated based on quantum communication, information and computation methods [7–10, 44], Secs. 2–5.

In step 7, Bob's energy state can continue to lower due to energy loss or a photon number splitting (PNS) attack by Eve [31–34], as a *poor imitation of a prize state* denoting some of the prize energy. From [6, Sec. 8.2], a PNS by Eve at a beam splitter operating on a BEC [56], can be adapted as photonic detectors/probes (steps 5–7) observing events on a BEC scale to share information [7, 58, 59, e.g., *qudit communication*] over the quantum channel between Bob, Alice, and the boxes. At step 6, Eve or Alice keeps one portion of the information about the quantum particle while the other portion is given to Bob (step 4), as any of the three parties interact with the quantum particle and its boxes.

In the QDF model, Bob can win the prize from a box by obtaining the quantum information [7, 10, 33, 37] about the prize. This information is based on four measurement variables (fmv). One variable is the prize position $\mathfrak{r}$, [15]. The second variable is an interaction length-based scalar κ that provides information on the expected TS (or game outcome, Appx. A). This scalar is generated from N-participant interactions [42] over a distance d (a scalar quantity). The third variable is a pairwise interaction distance of $2d/3$ between Bob and a participant relative to the prize position $\mathfrak{r}$. The prize is somewhere at distance $d \to |\mathfrak{r}|$ measured between three boxes (steps 1–4) down to two boxes $(2d/3) \to |\mathfrak{r}|$ (steps 5–7), in order to find $\mathfrak{r}$ by Bob. Distance d transforms into $|\mathfrak{r}|$ if, and only if the magnitude of the change in the interaction distance $|\Delta d|$ is applied between d and the fourth variable. The fourth variable is the correlation length λ_c between the state of a pair of interacting participants and the state of a box resulting from a state transition (ST) that occurs inside a box. The relationship between the fmv components is discussed in Sec. 4.

An ST denotes the state of a box without a prize, with a prize, or both in case of superposition. Eve's information on the state of being with and without a prize will not necessarily allow Bob to win the prize as his TS. From this superposition, the probability of Bob predicting the box having the prize is reduced from $1/2$ to $\leq 1/3$ due to m number of possible quantum states that can occur in a box. This occurrence is at a distance ratio of $d/3m : d/2$.

Particle superposition becomes entanglement [26], if Bob acquires the state of a box at a distance $\geq 2d/3m$. The condition for Bob is to find his TS via Eve at what point Alice transfers the state of the prize from one box, as the sender, to another, as the receiver [26, 37]? This observation is made on the prize's *quantum state teleportation* between boxes and a participant, as in e.g., between BEC EPR (Einstein-Podolsky-Rosen) pairs [55–57], or network nodes [7, 25, 26, 36]. Therefore, Bob can assume m quantum states characterized by the principal quantum number, as any interacting participant during quantum state transfer between boxes. In this paper, terms like "momentum transfer" from one particle to another denote the same "state transfer." This quantum state transfer between e.g., qubit pairs has been discussed and implemented with results and analysis in [7, 9].

A BEC experimental model [61–67], e.g., a thermal BEC black hole [22–27], can provide information and predict how a GS or ES particle pair get entangled on a scale of Planck length $\lambda_P \approx 10^{-35}$m. The length value can be used as

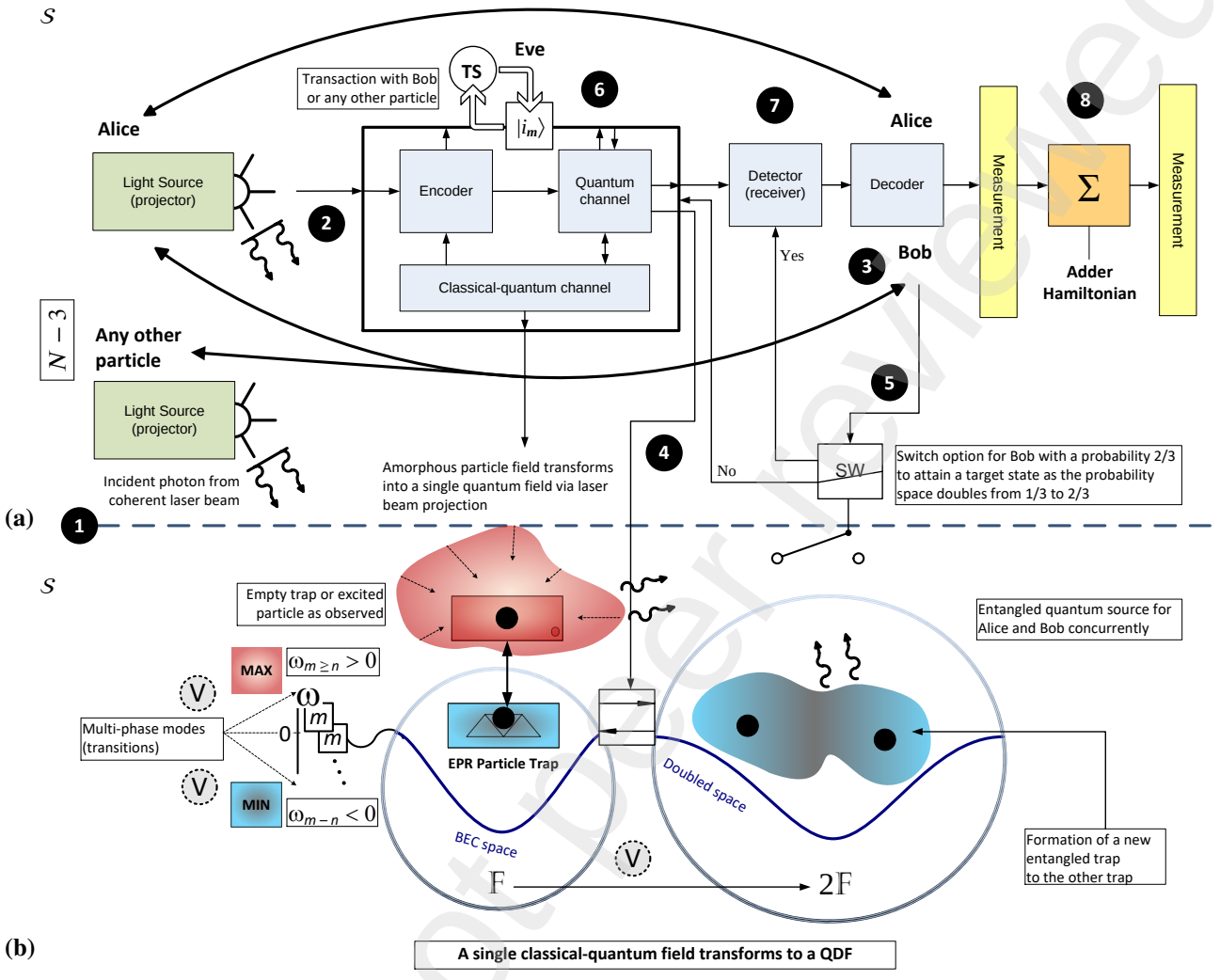

Fig. 1: **(a)** QDF model and circuit with Alice, Bob, Eve and $N-3$ particles presented as their energies exchange between steps 1–7 to share, hide, predict or gather information on the prize position $\mathfrak{r}$. The sum of losses and wins for a particle of the QDF circuit is measured at step 8. The model thermodynamics can be mapped from the model steps by particles interacting in the system. A particle inputs energy and interacts with another particle resulting in an energy output in $\mathcal{S}$. In a quantum game, as proposed in Appx. A, the input can be a *suggestion* by a participant causing *a switch* by Bob as his *decision* during communication. **(a)** and **(b)** A classical or quantum measurement can be done on system space $\mathcal{S}$ [73], and Bob is in $\mathcal{S}$ an atom exchanging energy with others. **(b)** left side, corresponds to possible PTs between a CPT and QPT as a particle traps within a GS, with a probability 2/3 for Bob winning a prize at the switch, **(b)** right side. **(b)** left-to-right image, the classical-quantum channel corresponds to the frame of reference of doubling the field $\mathbb{F}$ with a probability 8/9 to 1 of winning the prize (to validate, see Sec. 7 proof, or Eq. (53)). This channel corresponds to **(a)** and **(b)**, as quantum events take place against Bob due to Alice's TS quantum abilities. For example, the creation of EPR BEC pairs is followed by a QKD versus a PNS attack, steps 4–6. See, Sec. 2.2 and Fig. 6.

a *boundary indicator* to observe and compare micro and macroscopic events limited to Bob's energy state in winning the prize, once he is paired and entangled with the prize, as opposed to a GS matter (GSM, or a/no prize), [7, p. 6].

A BEC from Fig. 1(b) approaching singularity as a dense mass formation at $d \in (1, \infty]$, relative to λ_P, is Bob's decision point or switch. From the mass-energy equivalence [44], given the dense mass, our model focuses on the varying degrees of energy transfer to Bob. This accounts for energy dissipation in the system [44, Sec. 2.3], if he only wins a prize, as opposed to winning the prize as his TS (steps 7 and 8). Here, discrete GS levels of energy are predicted

by forming a BEC, or a GS cold atom in a trap (box) [39–41, 55, 90], in a QPT. The means to produce this event is via photonic projections by Alice with the focus on momentum transfer and readout of a trapped atom and Bob's state. The CPT, or a crossover from a QPT to a CPT for an ES, occurs at $d \in (\lambda_P, 1]$, Sec. 6. Our model can benefit from BEC models to determine the prize win probability for Bob, Secs. 2–8, or see the validated results from [7].

The QDF participants interact and exchange quantum information [33] in steps 4–7. Bob uses the information to continue his interactions with the initial box or switch to the other box. In a QDF game, Figs. 6(c)–(e), as in other games [14–16, 19, 20, 68, 69], Bob has to make a decision (to *switch?*, Fig. 1) based on superposition or entanglement of his state with the prize determined from their λ_c [35, 41].

The QDF system model benefits from the QKD (quantum key distribution) [31, Sec. 12.6], EPR and PNS attack models, Figs. 1, 6, [31–34]. The stronger the correlation between particle states observed by computing the fmv, the greater the entanglement between the particles, as in Bell states [12, 31]. One quantum particle as the prize, and a classical particle without any quantum ability as Bob, can entangle via Eve and become a paired quantum particle. This requires Eve to interact with the prize, sharing the quantum information about the prize with Bob. However, if Eve and Alice observe $\mathfrak{r}$, while not sharing information about $\mathfrak{r}$ with each other, the correlations between the prize momentum and $\mathfrak{r}$ may not exceed a value of 2, as in Bell's inequality [29–31]. From the interaction between a pair of participants, e.g., Bob with Eve or Alice, the outcome of Bob's measurement on $\mathfrak{r}$ depends on Eve or Alice's measurement, which predicts the system model outcome by violating Bell's inequality [32, 46]. Bob via Eve stays connected to the prize as the prize superposes in step 6, until he makes a decision at step 7.

A *cheap prize* or a *poor imitation of the prize quantum state* (*some of the prize energy is absorbed or received*), can be traced between its positions as it superposes, according to the PNS attack, Figs. 1(b) or 6(e). The notation $\bigvee$ is a disjunction between two or more prize positions relative to its quantum states denoting the prize to be in one of the boxes with a probability of the mth state equal to $2/3m : 1$. As far as Bob stays entangled with the prize via Eve, given the information gathered by her from the trace, the greater the probability of winning a/the prize by Bob. This occurs at steps 6 and 7, which conforms to the entangled QKD model as e.g., an entangled EPR pair, Secs. 2–4.

Remark 1. The poorest prize imitation in a PNS attack can equate to the energy state revealed from the opened box by Alice at step 4, nearing 0 (a GS sublevel, Sec. 2). In the CPT model, this is visible to all participants as no prize. In the QPT model, a closed box between steps 5 and 7 can denote an empty box, no prize, a prize, or the prize.

In Secs. 2–6, the CPT and QPT models are used to characterize a thermodynamic system. A system observer gathers the fmv-based information via quantum measurement to determine the outcome of each ST for a TS [78–81], as a prize win or loss. Sections 7–9 present the proof and application of the QDF model, followed by final remarks.

2. State transition models

A PT at a critical point (temperature) of the system is reached after a series of STs, which are from Bob's interactions with other participants, each having their own energy input E_{in}, Figs. 1(a) left to 1(b) left. The expected value of STs out of all interactions, is the expected energy output $\langle E_{out} \rangle$ as a PT at step 7 (or see Fig. 6). This PT presents the complete picture of a prize state and all of the states of the participants as the system event outcome (system state).

There are two ST models presented here that are linked after determining the values of fmv of the system. Section 2.1 presents the classical model which describes a PT based on STs as events with some probability. Section 2.2 presents the quantum model, where the fmv approximates any ST probability to a particle entanglement outcome between pairs relative to their energy input. This is by coupling the input state (as a quantum or classical state) with the output state denoting the classical prize state based on Fermi's golden rule [80], as discussed in Sec. 6.3. This model predicts a classical outcome with certainty by measuring quantum product states (qubit pairs), distinguishing Bell states between particles. The statistical data are provided in the method article [7, 9], proving the *universality* of the QDF model for a set of CPTs and QPTs observed in a system, i.e., the sum of step 8 readouts in Fig. 1(a).

2.1. Classical model

The system thermodynamics can be mapped from the steps played by participants from Fig. 1 or 6 as particles interacting within space $\mathcal{S}$. A participant inputs energy E_{in} (a suggestion or decision by interaction), and interacts with another participant resulting in an energy output E_{out}. In $\mathcal{S}$, Bob is an atom exchanging energy with other participants.

State i from an ST can occur inside a box. The classical GS $i = 0$ denotes the prize is not present. The ES $i = 1$ denotes the prize is present. The prize in this model is an exciting particle. If Bob chooses (interacts) with the box having the prize, *his state becomes the exciting particle state*.

The participants can interact continuously. Bob continues losing energy to other participants, as he keeps interacting or choosing the box with no prize, else he gains energy by winning one or more prizes. This is a continuous PT [78–80], as state $i = 2$ denotes a box continuously with a prize in one game and without in a new game, i.e., between step 7 of the current game, and step 2 of the new game. Here, Alice can change the value of prize position $\mathfrak{r}$ in step 1.

In this model, Bob's energy loss in $\mathcal{S}$ is to other participants and not the prize, where all energy states are distinguishable. This has a statistical significance in calculating the expected energy output $\langle E_{\text{out}} \rangle$ relative to E_{in} from their momentum and position field variables. In a PT, under a scalar field transformation, the output of all the energies from participants with the prize can scale up to the system's total energy E, see Eq. (8) for comparison.

The pairwise interactions continue as a participant loses energy to the other and so on, until an energy amount is returned. Here, Bob receives information from participants and keeps losing the game until he wins a prize. If the observation from e.g., Eve correlates to Alice's information about $\mathfrak{r}$, and shared with Bob in a particle pairing process, Bob's energy increases to an excited state like the prize as his TS, Sec. 4.2. This establishes the quantum model below.

Remark 2. In the classical model, there is no prize from observing a GS and no information, or zero entropy. The result remains 0, even if Bob interacts multiple times playing this game in a loop, repeating all model steps. Hence, Bob's energy loss is to other participants and not to the prize, where all of their energy states are distinguishable.

2.2. Quantum model

The QDF model attempts to represent high and low energy physics on any observable scale of the universe via scalar κ associated to the QDF metric space, as discussed in Sec. 4. Two pictures of this model are presented. In either picture, a particle in the QDF model can exchange roles with:

1. Any particle that exists at a *quantum measurement point*, i.e., a sample of space $\mathcal{S}$, is identified and chosen for determining the fmv. This point is scaled between any of the given inputs and expected outputs of the fmv. The value of this point as chosen in each projected picture, denotes the observable of energy, momentum, position, etc., as a measured property of a particle in $\mathcal{S}$, which is further discussed in Sec. 3.
2. A particle that is chosen from the quantum measurement point, given its expected *quantum readout point*, which changes and scales between one or more expected outputs, and determines a model step outcome.
3. A particle that physically behaves differently in a different energy state e.g., atoms that behave like a boson as a composite body of fermions, such as a BEC of ultracold ^{87}Rb atoms near 0K temperatures.

The identification of these quantum measurement and readout points defining the outcome of each picture is discussed in Sec. 3. These points can represent a particle, an event, an ST, TS, a QPT, and mimic e.g., the conversion of light into subatomic particles as a matter-energy exchange at a critical point (or PT). Some examples are pair-production and conversion of particles discussed within a quantum field theoretical context [52]. These points can be chosen to observe and predict events prior to a PT. For example, a BEC or a GS cold atom (GSM) is produced in a trap (box) through laser cooling [1, 38, 54, 55, 90], or methods of GS population trapping [60], where quantum information is stored and read from the atom. Once the laser beam(s) and magnetic field keeping the atom in a trap are turned off, a particle with momentum is released from the trap [1, 33, 54]. This is where there is no trap, since BEC in Fig. 1(b) occurs below a critical temperature, role #3 above. The production of BEC from a GSM in a correlated system is discussed in Sec. 4.1.

From a statistical thermodynamic viewpoint, the role of a particle can change, given its quantum measurement and readout points, characterizing an energy component of the system's total energy or Hamiltonian. This is satisfied by e.g., a spin-lattice model trapping particles [39–41] to produce a GSM which can scale and transition into a BEC.

2.2.1. Probabilistic picture

In this picture, Alice in space $\mathcal{S}$, is at one of the quantum measurement and readout points representing a particle as a projector, observer, etc., relative to the other point where the prize or Bob is, roles #1–3. The prize is a *quantum particle*. Alice is a *photonic probe* (in short, a *photoprobe*) reading Bob's state. For example, a photoprobe observes a photon from a scattering event at a pairwise particle interaction site [7, 53, 93]. Alice measures the energy state at

this pairwise point, or the area of boxes (particle traps), Figs. 1 and 6(b), which carries the frequency of the pairwise interaction during a scattering event. This measurement is described by an ST operator $\mathcal{T}(i)$ in Eq. (1a), or see Eq. (6) for the scattering event. The sum of interactions between Alice, Bob, and the prize, represents this event. Alice can also project her energy state onto Bob's space as a photon from a coherent light source (a pump laser as the source of photons in a BEC experiment [62]). This is the quantum information as qubits that can be read from trapped atoms [54, 55]. A particle of $N-3$ particles in Fig. 1(a), as an *audience member* in Fig. 6, is a photon, randomly projecting an energy state from the light source. The prize position $\mathfrak{r}$, is difficult for Bob to predict, as Alice can switch the prize between boxes (steps 1–6). This can be described by producing BEC EPR pairs [56, 57], Example 2. Alice measures the energy state at a pairwise point or area occupied by Bob and the prize, which carries the frequency of the pairwise particle interaction site [7]. This is due to setting up a quantum state $|i\rangle = |2\rangle$, which denotes a box prior to decoherence, as a combination of with and without the prize during the game.

Alice via photonic projections superposes the prize in its position space $\mathcal{S}_{\mathfrak{r}} \subset \mathcal{S}$. This superposition is decomposed into a vector sum of the $\mathfrak{r}$-based field

$$\Psi(\mathfrak{r})\,|\mathfrak{r}, i\rangle = \sum_{\mathfrak{r}} \psi_0(\mathfrak{r})|\mathfrak{r}, 0\rangle + \psi_1(\mathfrak{r})|\mathfrak{r}, 1\rangle + \psi_2(\mathfrak{r})|\mathfrak{r}, 2\rangle, \tag{1}$$

where $\psi_i(\mathfrak{r}) = \langle \mathfrak{r}|\psi_i\rangle$ is the probability amplitude describing the particle position $\mathfrak{r}$ and quantum state

$$|i\rangle = \{|0\rangle = \left[\begin{smallmatrix}1\\0\end{smallmatrix}\right], |1\rangle = \left[\begin{smallmatrix}0\\1\end{smallmatrix}\right], |2\rangle = \overbrace{\left[|i_m\rangle \otimes (|0\rangle + |1\rangle)\right]}^{[|i_m 0\rangle + |i_m 1\rangle]} \overset{\mathcal{T}(i)}{\longleftrightarrow} |i_m\rangle; i_m < 2\}, \tag{1a}$$

given that $\mathcal{T}(i)$ is the ST operator satisfying a transition from a Schrödinger's cat state to state $|i_m\rangle$, and its reverse. The Schrödinger's cat state can undergo a transformation via $\mathcal{T}(i)$, where entangled states are built with orthogonal states of Bob and Alice, e.g., $|01 + 10\rangle$. This operator can be interpreted as a translation, spin, momentum or rotation operator acting on a particle at $\mathfrak{r}$, satisfying an ST. Entanglement can be expressed as a tensor product *distributes over superposition* [11], $|i_m\rangle \otimes 2^{-1/2}(|0\rangle + |1\rangle) = |2\rangle$. An ST for $|2\rangle$ as $|0_m\rangle$ occurs within state $|0\rangle$ as a QPT, i.e., an atom in condensate [7, 78–81]. This can be a macroscopic superposition of two degenerate GSs where a probable entanglement can be extracted [28, 45]. However, the state $|2\rangle$ can be a continuous QPT crossover to a CPT [77–81]. The QPT and its crossover condition is denoted by $|i_m\rangle \to i$, [83–85], where $|0_m\rangle$ and $|1_m\rangle$ are, respectively, GS and ES lower or higher mth energy level, Fig. 1(b). This can be shown by an ST operation $\mathcal{T}(i)|i_m\rangle = |i \times i_m\rangle = |2\rangle$, which denotes infinitesimal shifts within the GS, yet with the possibility to crossover from $|i_m\rangle$ to a classical excited state $i = 1$. An example of using this model is further discussed as decoding a Schrödinger's cat state into classical states in the method article [7, Example 4], or see Remark 8 examples.

Remark 3. Classical state $i = 0$ is a number as matrix element $i_{11} \in |i\rangle$, and $i = 1$ as $i_{21} \in |i\rangle$, for a CPT. Quantum state $|i\rangle$ is contained within each matrix as an ST occurs for a QPT, otherwise its crossover to a CPT by $\mathcal{T}(i)$.

Remark 4. Hereon, from Eq. (1a), the probabilistic expected value of $|2\rangle$ measurement in equations will be self-contained, including degrees of superposition, such as an equal superposition of $2^{-1/2}(|0 + 1\rangle)$ having equal probabilities $|2^{-1/2}|^2 = 1/2$ for being 0 and 1. The state can be interpreted via $\mathcal{T}(i)$ which provides the specific expected value in this picture, see Eqs. (1b), (1c), and Example 6.

Eve carries information from Alice as an observer collecting energy like a photoprobe (step 6). Eve at a quantum measurement point, is an atom, a photon or a photoprobe. Eve's field as a photoprobe and a photon, can exchange energy with Bob to provide information on Alice's state and the prize. If Eve interacts with Alice's field during superposition, then Eve is also superposing between Bob, Alice and the boxes. Eve can share information about the prize with Bob via energy projections onto his field, after collecting information from Alice and the boxes. If Bob via Eve transforms his field into Alice's field to superpose, he wins. The reason is, his field via κ collapses to Alice's field, and so obtains her TS information. As Bob reveals his TS (step 7), *quantum decoherence* occurs, revealing one of the quantum states as a classical state $i = 0$ or 1 from the box.

For Alice, Bob, Eve and/or the audience, the locally indistinguishable Bell states in $\mathcal{S}$, can be written as a set of distinguishable Bell states by adding an extra qubit from Eve, $|2\rangle_{\text{Eve}}$. This is presented in its tensor product form as

$$\overbrace{|2\rangle_{\text{Box}}|2\rangle_{\text{Alice}}|2\rangle_{\text{Bob}}}^{\text{indistinguishable}}\otimes|2\rangle_{\text{Eve}} = \overbrace{|i_m\rangle_{\text{Box}}|i\rangle_{\text{Alice}}|j\rangle_{\text{Bob}}\mathcal{T}(i)|i_m\rangle_{\text{Eve}}}^{\text{distinguishable}} \tag{1b}$$

product states, where $j(j \leq i) \in [0, 2]$ is the state of a particle interacting with Bob, changing his state in $\mathcal{S}$, Sec. 4.1. These are qubit states *mimicking Bell states without entanglement* [18, 55] as quasi-Bell states, that possess orthogonal and nonorthogonal states. The tensor product of Eve's state is vital to reveal the state of the box inside from $|2\rangle$ to $|i_m\rangle$ by the ST operator $\mathcal{T}(i)$, which transfers the state to Eve as $|i \times i_m\rangle_{\text{Box}} = |2\rangle_{\text{Eve}}$. The probable outcome of this ST denotes state $|2\rangle_{\text{Eve}} = |i_m\rangle_{\text{Box}}$ set up by Alice is known to her as $|i\rangle$. This reveals with certainty the prize state for that box, according to Alice and Eve. In this relation, Eve is always needed to communicate the result to anyone else.

This picture has two bits of information hidden in the QDF circuit, and with an extra qubit in state $|2\rangle$, the circuit reveals the information, Fig. 1(a). From Eq. (1b), the model predicts pure, distinguishable, orthogonal and separable states in all cases [7, 18]. For instance, the Schrödinger's cat is in a superposition state like the prize in a box, and not necessarily entangled. The photon set up by Alice (observed by Eve) as the light source projecting randomly polarized light onto the particle in the box, is in a mixed state. This can be the cat as a trapped BEC or a GS cold atom Fig. 1(b), or [7]. However, the cat, Alice, Eve, and their environment *together*, are in a pure state as we construct a product of their states, Eq. (1b). Hence, an extra qubit as physically part of the QDF from its metric space, Sec. 4.2, is required from Eve to render distinguishable states and avoid any information loss from decoherence, see Remark 5.

2.2.2. Deterministic picture

In this picture, an atom is framed as Bob, and an atom in a multilevel trap (box) is the prize paired with Bob's state returning their product state via laser cooling [41, 55]. The laser could be Alice with a storable qubit state on a lattice site denoting the prize state. The QDF model, Fig. 1 as a thermodynamic system can benefit from a spin-lattice Ising model, laser cooling, and quantum field components. In this model, qubits are read from trapped atoms in condensate, e.g., BEC [55]. The thermodynamics of the quantum information and entanglement between BEC atoms, in form of EPR pairs [55–57] as photons project, absorbed (laser cooling) and re-emit (as detected by photodetectors) among pairs, are presented in [7]. This model applies to a set of n sampled particles trapped in the system $\leq N-n$, as quantum particles with different prize states in the game. The inequality returns $2n \leq N$, which links the n sampled particles to $2n$-EPR pairs between their traps and/or lattice sites, as entangled qubits [7, Defs. 4d, 4e, and Eq. (31)].

Quantum decoherence is the focus on the statistical prediction side of quantum events (system's measurement outcome), where the ST probabilities associated to e.g., EPR pair creation, teleportation and *superdense coding* [44, Chap. 13], are based on knowing parts of a communication or a message exchanged between Alice, Bob, Eve and the audience in a QDF circuit [7]. This is visible within the quantum communication protocols [44] of a QDF circuit based on particle pairing and entanglement, Sec. 4.2. For example, an extra qubit can be used to denote Eve's state, or a qubit pair for her to entangle as the vital party and physically part of the QDF metric space. This is expressed by

$$|ij\rangle_{\substack{\text{Alice}\\\text{Bob}}}\otimes|2i_{\mathcal{S}}\rangle_{\text{Eve}} = \overbrace{\left(|0_m i\rangle \pm |1_m i'\rangle\right)_{\substack{\text{Alice}\\\text{Bob}}}}^{\text{indistinguishable}}\otimes|i_m i_{\mathcal{S}}\rangle_{\text{Eve}} = \overbrace{\left(|0_m i\rangle_{\substack{\text{Alice}\\\text{Bob}}} \pm |1_m i'\rangle_{\substack{\text{Alice}\\\text{Bob}}}\right)\mathcal{T}(i)|i_m i_{\mathcal{S}}\rangle_{\text{Eve}}}^{\text{distinguishable}}, \tag{1c}$$

where i' is the negation of i as the target qubit, which flips if $i_m = 1$, and $|i_{\mathcal{S}}\rangle$ is a qubit state produced in space $\mathcal{S}$ for Eve from a particle interaction. This state when coupled in its tensor product space, produces locally distinguishable states. Eve's states complement the states of other parities such as Alice, Bob and the prize, generating distinguishable Bell states. This process eliminates a set of indistinguishable states via Eve's qubit pair as an EPR pair, communicating the result to anyone else. In a given model step, it is expected that the prize is either entangled or in superposition. The pair of qubits from Eve hold nothing of local value and only global, since her states are all nonorthogonal. Locally, Eve is vital to reveal the hidden information to Alice, Bob or Eve as the expected output state of the system. This establishes the deterministic picture, which shifts back to the probabilistic picture from superdense coding [7] as the inverse of teleportation. In this process, the EPR source is shared to decode events in classical bits of information.

Remark 5. In the deterministic picture, the limitations from the uncertainty of measurement points are not applicable to correlated systems of e.g., $2n$-BEC EPR pairs. The focus is on the superposition of quantum measurement points relative to a broad range of readouts of entangled states. For instance, product states entangled with Eve's extra qubit can correct or avoid information loss from decoherence with the environment. This qubit can be used to encode product states of Eqs. (1b) and (1c), into an entangled state of $3[n, 2n]$ physical qubits to correct a qubit error [7, 44].

3. Quantum measurement

In the classical model, Sec. 2, a sample of $\mathcal{S}$ has mutually exclusive possibilities, only one of which is to take place in a particular model step. In the quantum model, a sample of $\mathcal{S}$ is always a *projective decomposition of the identity* (PDI) *of outcomes*, and not the identity of probability distributions [73, 74], of the same model step.

There are two measurement problems in this paper:

1. Measurement outcomes given the physical quantity of $\mathcal{S}$ which form a PDI through a projector.
2. Measured properties of any particle in $\mathcal{S}$ are observables based on the fmv components, Sec. 1.

Note that for each measurement, the probabilities associated with its outcome need to be calculated [74, 75]. The corresponding solutions are:

1. Project a state in the direction of another state (a pointer) in a definite position.
2. Conclude from the definite position a *prior value* [74] before it is influenced by a photon or photoprobe (e.g., Alice) before measurement.

A sample of $\mathcal{S}$, the relevant PDI choice, and the fmv-based properties of a particle before measurement, are the tools to solve measurement problems within a model step.

To solve problem 1, a quantum measurement is conducted on a particle as Bob, where a photoprobe (Alice or Eve) interacts and gives a measurement outcome. The probability of the outcome is estimated with some uncertainty on the classical state of the prize which is the quantum particle. The photoprobe and the prize are (pointers) in superposition relevant to a model step. The prize has a definite position only if its information (momentum) is transferred to the atom Bob, as the solution to this measurement problem. The *identity* is the *sum of projectors* [74] on $\mathcal{S}$, giving mutually exclusive possibilities, one of which is true, Sec. 4.1.

To solve problem 2, a quantum measurement is conducted on atom Bob, where photoprobe Alice via photons interacts and pairs up, Sec. 2.2.1. In the QDF metric space via particle pairing, PDI is used through QDF projectors as a solution to this problem. Alice's field and the prize are superposed or entangled with Bob as a pair and satisfy a QDF transformation relevant to a model step. The problem is solved by having the information from the pair which contains the prize position value, a "prior value" for Bob to switch. This is the property of the prize before measurement.

A compatible measurement [74, 75] is obtained on Bob who assumes or expects $\langle \mathfrak{r} \rangle$ from his position $\mathbf{r}$ relative to $\mathfrak{r}$ as $|\langle \mathfrak{r}\mathbf{r} \rangle|^{1/2}$ via photoprobe's momentum observation. The momentum is observed from the probe's photon field relative to Bob's field. This requires a *joint correlation measurement* of pairwise observables conducted on a particle pair, as their states couple between input E_{in} and output E_{out} in $\mathcal{S}$ under a QDF transformation. This transformation is expressed by QDF projection products that switch the system state (a PT). This transformation is satisfied by a κ-based field switch function $f(\kappa)$ in a QDF circuit, Secs. 5 and 6. Consequently, the prize momentum is transferred to the superposing particle in a pairwise interaction with its pair sharing the value of $\mathfrak{r}$ with Bob before a switch, Fig. 1. These κ-based field expected outcomes should be consistent with the history of compatible (projective) measurements of space $\mathcal{S}$. This history can be validated by classifying states from qubit-to-classical data, using quantum AI [7, 8].

The measurement on the photoprobe momentum, prize position $\mathfrak{r}$ and its expected position $\langle \mathfrak{r} \rangle$ assumed by Bob from his position at $\mathbf{r}$, and the projection of fmv outcomes under a QDF transformation, are discussed in Secs. 4–6.

4. QDF metric space and transformation

Firstly, to construct the QDF metric space and transformation, the single-field transform must be defined, Sec. 4.1. Secondly, the QDF transform via particle pairing must be defined, Sec. 4.2. Lastly, a strong state prediction via PDI can be made based on Secs. 5 and 6 outcomes, followed by the QDF game, application, proof and theorem in Sec. 7.

4.1. The single-field transform

Bob's field Ψ is based on position space $\mathcal{S}_{\mathbf{r}}$, where $\mathbf{r}$ is his position relative to position $\mathfrak{r} \in \mathcal{S}_{\mathfrak{r}} \subseteq \mathcal{S}_{\mathbf{r}\mathfrak{r}} \subset \mathcal{S}$, which form a prize interaction area $|\mathbf{r}\mathfrak{r}|$. By projecting photons, his field can transform into Alice's field as a photonic field Φ based on momentum space $\mathcal{S}_{\mathbf{k}}$, where $\mathbf{k}$ is the wavevector describing a photon and its momentum. Notably, the measurement of wavenumber $k = |\mathbf{k}|$ is equivalent to a measurement of the particle momentum [92].

Alice's field can carry the average particle momentum relative to its position $\mathbf{r}$, or equivalently, frequency [72]. This is based on the position-momentum correlation $\langle \mathbf{kr} \rangle_{\mathrm{c}}$ of space $\mathcal{S}$, which measures the expected values $\langle \mathbf{kr} \rangle$ of a system state $|\Psi\rangle$ or $|\Phi\rangle$ in finding $\mathfrak{r}$. This measure is made relative to the uncertainty measure of $\mathbf{k}$ and $\mathbf{r}$, i.e.

$$\langle \mathbf{kr} \rangle_{\mathrm{c}} = \left(\langle \mathbf{kr} \rangle - \langle \mathbf{k} \rangle \langle \mathbf{r} \rangle \right) / \mathbf{k}_{i,j} \mathbf{r}_{i,j}, \tag{2}$$

where $\mathbf{r}_{i,j}$ and $\mathbf{k}_{i,j}$ are, respectively, the change or uncertainty in particle position and momentum, and $j (j \leq i) \in [0, 2]$ is the state of a particle interacting with Bob, increasing or lowering his energy. States i and j have, respectively, wavevectors $\mathbf{k}_i$ and $\mathbf{k}_j$, and positions $\mathbf{r}_i$ and $\mathbf{r}_j$. Hence, components $\mathbf{k}_{i,j}$ and $\mathbf{r}_{i,j}$ can be written as

$$\mathbf{k}_{i,j} = \left| \mathbf{k}_i - \mathbf{k}_j \right| \qquad \text{and} \qquad \mathbf{r}_{i,j} = \left| \mathbf{r}_i - \mathbf{r}_j \right|. \tag{3}$$

The change in momentum and position can be, respectively, interpreted as the square root of their variances $(\langle \mathbf{k}^2 \rangle - \langle \mathbf{k} \rangle^2)^{1/2}$ and $(\langle \mathbf{r}^2 \rangle - \langle \mathbf{r} \rangle^2)^{1/2}$, or a standard deviation. The average of the absolute deviations from the N participants' shared information about $\mathfrak{r}$ can be shown by adapting the indices to the area of pairwise particle interactions. This gives the average change in momentum and change in position in each particle site relative to its pair as

$$\langle \mathbf{k}_{i,j} \rangle = \left| \frac{1}{N} \sum_{i=0}^{N-1} \mathbf{k}_i - \frac{1}{N} \sum_{j>i}^{N} \mathbf{k}_j \right| = \frac{\left| \mathbf{k}_i (N-i) - \mathbf{k}_j (N-j+1) \right|}{N} \quad \text{and} \quad \langle \mathbf{r}_{i,j} \rangle = \frac{\left| \mathbf{r}_i (N-i) - \mathbf{r}_j (N-j+1) \right|}{N}. \tag{4}$$

The momentum transfer from a particle to its pair with lower energy can result in a PT as $[\mathbf{k}_{i,j}^2]^{1/2} < \lambda_{\mathrm{P}}^{-1}$, [63], which is discussed in Sec. 4.2.1.

Remark 6. In the quantum model, i and j values are limited to $[0, 2]$, where the value 2 denotes any GS or ES of a particle's quantum state $\mathcal{T}(i)\{|0\rangle, |1\rangle, \ldots, |N-1\rangle\} \mapsto |2\rangle$, where the ST operator maps superpositions of N states via $j \in |ij\rangle \rightarrow \mathcal{T}(i)|i_m i\rangle$. This determines a QPT or a crossover to a CPT, see Eq. (3), Example 1 and [7, Eq. (35)].

The uncertainty relation (HUP) for $\mathbf{kr}$-quantum observables derived for the standard deviation in Eq. (2) is

$$\mathbf{k}_{i,j} \mathbf{r}_{i,j} \geq |\langle \Phi | \mathbf{kr} | \Psi \rangle| / 2, \tag{5}$$

where Φ in the bra $\langle \Phi|$ can be replaced with Ψ in the ket $|\Psi\rangle$, or vice versa, depending on the direction of projection of a state, from or to the prize, or from one participant to another. The outcome of the inner product defines the system state [87]. For instance, if the lower bound is $|\langle \mathbf{kr} \rangle| \rightarrow 0$ with system state $|\Psi\rangle$ or $|\Phi\rangle \rightarrow 0$ expectation, then the probability of finding a particle at the measurement point is low or a weak HUP [88, 91]. However, if the system state is projected as $|\Phi\rangle \rightarrow 1$ from $|\langle \Phi | \Psi \rangle| \neq 0$ onto $\mathcal{S}$, then the expected measurement outcome is from incompatible observables and wavefunctions (nonorthogonal), Secs. 3, 5, [74]. The measurement of these observables as $\mathbf{k}$, $\mathbf{r}$ and $\mathfrak{r}$ in $\mathcal{S}$, to a compatible measurement of $\mathfrak{r}$, is only if $\mathfrak{r}$, $\mathbf{k}$ and $\mathbf{r}$, are mutually correlated, Sec. 3. This denotes three correlated observables under the transformation $\Psi \rightarrow \Phi$ by a κ-based field operation, Eq. (6), where the exponential in Φ is approximated by unity $e^{i\mathbf{kr}} \approx 1$ at a readout point.

An example for such transformations would be the wavelength of a radiation emitted in an ST, provided by a scalar product operation $|\kappa^2| \lambda_{\mathrm{c}}^{-1} = \mathbf{k}_{i,j} |\mathbf{r}|$ for a PT, Sec. 5. Let us assume that the wavelength of a BEC atom (of a BEC EPR pair) is large compared to $d = |\mathbf{r}| > 0$ at one of the expected readout points $\mathbf{r}_i$ from the pairwise interaction area $|\mathfrak{r}\mathbf{r}|$, where $\sqrt{|\langle \mathfrak{r}\mathbf{r} \rangle|} \rightarrow \mathbf{r}_{i,j} \leq |\kappa^2| (\lambda_{\mathrm{c}} \mathbf{k}_{i,j})^{-1} = d$. Here, the wavefunctions Ψ and Φ restrict the effective values of $\mathbf{r}_i$ to $\mathbf{r}_{i,j} \lesssim d$, so that $\mathbf{k}_{i,j} \mathbf{r}_{i,j} \lesssim kd = |\langle \mathbf{kr} \rangle| \gtrsim 0$. In this case, the probabilistic picture of this event shifts to zero uncertainty in the deterministic picture, Secs. 2.2 and 5.3.

In both pictures, projection-valued measures (PVMs) between participants and the prize can be stored as a system measurement outcome in $\mathcal{S}$, as in [10], where the number of Hilbert space dimensions can be defined as the number of

storable data points L_d in [7, Eq. (28)]). This is satisfied by QDF *interaction operators* acting on two-qubit registers [7, Eqs. (25)–(36)]. The QDF information obtained from these qubit registers is decoded as classical information based on Bob and Alice's momenta spread in their frame of interactions (observation) [10, pp. 3–10]. Each register can be served as a memory providing information on $\mathbf{k}$ and $\mathbf{r}$ to Bob via his interaction with Eve, who measures $\mathbf{k}$ and $\mathbf{r}$ in her frame from the boxes to Alice, Secs. 4.2, 5 and [7, pp. 28–30, Example 5, and Meth. Valid. II].

Remark 7. In Eq. (5), $|\langle \mathbf{kr} \rangle| \to 0$, given the system state $|\Psi\rangle$ or $|\Phi\rangle \to 0$ expectation, breaks the ultimate minimum uncertainty as the HUP product to zero-valued bounds in the system. The standard deviations from Eq. (2) becomes ineffective to measure the uncertainty. Here, the quantum measurement points relative to readout points are shifted from measuring an HUP product in the probabilistic picture, to zero uncertainty in the deterministic picture.

In this paper, $\langle \mathbf{kr} \rangle_c$ is observed under a single-field or a QDF transformation ($\Psi \leftrightarrow \Phi$, defined in Sec. 4.2). Either field transform is associated with observables $\mathbf{k}$ and $\mathbf{r}$ as they correlate. These observables are characterized by their observable pairwise particle interactions that are interchangeably *replaced* by *particle pairwising* relative to d, e.g., Alice by Eve, Bob, This provides a simultaneous measurement of $\mathbf{k}$ and $\mathbf{r}$ of a particle pair relative to $|\mathfrak{r}|$ with minimum uncertainty, Secs. 4.2 and 5.

As discussed in Sec. 2.2.2, particle momenta of a pairwise field for an atom-atom entanglement, e.g., EPR pairs [7, 55–57], can be measured based on Eq. (4). This is to determine which states correlate as the pairs interact with photons from a light source (laser beam), and decelerate near 0K temperatures [54, 55]. In this scalar field, particles are trapped temporarily with a lifetime of a strong correlation between $\mathbf{k}$ and $\mathbf{r}$, as $|\mathbf{kr}| \to 1$. This occurs in a confined particle field (trap), where BECs or GSM are produced as a set of planewaves in a GS, with the limit $\langle \mathbf{k}_{i,j} \rangle_{|\mathbf{r}\mathfrak{r}|} \to 0$, Eq. (4), by incident photons from the laser beam on a scale of $\sqrt{|\langle \mathfrak{r}\mathbf{r} \rangle|} \to \mathbf{r}_{i,j} > 0$, Eq. (5), returning $|\langle \mathbf{kr} \rangle| \to 1$. However, the particles are accelerated or freed once the magnetic and laser fields are turned off, transforming the confined field to a free particle field, which scales to $|\langle \mathbf{kr} \rangle| \to 0$, expecting near zero correlations in $\mathcal{S}$, Eq. (2).

In Fig. 1(a), if Eve acts as a photoprobe, the particle's frequency ω is observed from the prize state relative to $\mathfrak{r}$ of a lattice site in Fig. 1(b), or [7, 72]. The photonic field can be from anyone else interacting with Bob as a photon with a probability amplitude $\phi(\mathbf{k}) = \langle \mathbf{k} | \phi \rangle$. This is a measurement of the photon momentum from a k-interval $\Delta k \in [\mathbf{k}, \mathbf{k} + \mathbf{k}_{i,j}]$, which is a momentum transfer from the photon to Bob that can cause his field to transform. A Bob-to-Alice field transforms as magnitude $|\mathbf{kr}|$ converges to a constant $|\mathbf{k}|^2 = 1$ due to a planewave travelling along $\mathbf{k}$, which reciprocally satisfies Bob's switch (decision) outcome in attaining his TS, Fig. 1(b) to 1(a). This convergence denotes the collection of all physical information by Alice from others about the prize position $\mathfrak{r}$, which is revealed after Bob's decision relative to his position $\mathbf{r}$. The magnitude of the information on where $\mathfrak{r}$ is, comes from those who interact with Bob and Alice, which is on a scale of $\sqrt{|\langle \mathbf{k}\mathfrak{r}\mathbf{kr} \rangle|}$ from their interactions, Sec. 5.3.

The transformation of a single-particle wavefunction from a GS to an ES is determined by the condensate density $\varrho(\mathbf{r}) = |\Psi|^2$. This satisfies the Gross–Pitaevskii equation [70, 71] describing a GS of Bob in a BEC, now into a TS of an ES as

$$\kappa^2 \Psi = \kappa^2 \sqrt{N \varrho(\mathbf{r})} e^{\imath \mathbf{k}_{i,j} \mathbf{r}} = \kappa^2 \psi_{i_n}(\mathbf{r}) \to \phi_{i_n}(\mathbf{k}) e^{\imath \mathbf{kr}} = \Phi, \text{ given } \left\langle \mathbf{k}_i \middle| \mathcal{T}(\mathbf{k}_j) \middle| \mathbf{r} \right\rangle = \psi_{i_n}(\mathbf{r}), \tag{6}$$

where $\imath$ is the imaginary unit, i_n corresponds to the nth participant (particle) who assumes (expects) state i in a box upon interaction, and ϱ determines the probability (density) that the particle in state i will be found at position $\mathbf{r}_i$ via $\mathbf{k}_{i,j}$, Eqs. (2)–(4). The transformation is reciprocal via a κ^{-2}-operation in Eq. (6), given the convergence for Bob by pairwising with participants on gathering information about $\mathfrak{r}$. The ES, $|i\rangle = |1\rangle$, can be determined by the double-field scattering factor $e^{\imath \mathbf{k}_{i,j} \mathbf{r}}$ of Alice's field Φ interaction. The photon propagation factor $e^{\imath \mathbf{kr}}$ is formed after $e^{\imath \mathbf{k}_{i,j} \mathbf{r}}$ (scattering) as translated by the space-time translation operator $\mathcal{T}(\mathbf{k}_j)$ at the interaction time with Bob's field Ψ. This satisfies photon integration in $\mathbf{k}$-space in a given magnitude between two pairwise interaction fields of Bob and any other participant. The GS $|i\rangle = |0\rangle$ can be determined via $\varrho(\mathbf{r})$ and the particle pairwising product to reveal $\mathfrak{r}$, Secs. 4.2 and 6.

Alice projects her state onto Bob's field, which is the information about showing a box that might have a quantum particle in a GS satisfying her TS (step 4). However, Alice shows an empty box ($i = 0$) as step 4 of a CPT model in a QDF game, Fig. 6, or an empty trap in Fig. 1(b). From Eq. (1), this photonic projection by Alice to Bob excites Bob to a higher energy state E_{i_m} via momentum transfer. This gives Bob some information about $\mathfrak{r}$ with a greater probability

to decide (to switch or not switch) where the prize is, as his TS (step 5). That is by knowing the box with no prize, which is a PDI of this model step measurement outcome via projection, as performed in a QDF circuit, Sec. 5.3.

If Bob obtains all the information about $\mathfrak{r}$ via interaction, then (after step ≥ 4), he can compute $\mathfrak{r}$ from the magnitude of positions $|\mathbf{r}| \rightarrow 2d/3 \rightarrow |\mathfrak{r}|$, where d is measured relative to $|\langle\Phi|\mathbf{kr}|\Psi\rangle|$. Possibly $\mathfrak{r}$ is found as the states are measured between Alice, Bob and the two boxes. In Fig. 1(b), the boxes can adapt to e.g., traps in a quantum oscillator [48–52, 61], satisfying a GSM in Fig. 4. Here, Alice has energy

$$E_{i_n} = E_0(2i_n + 1), \qquad E_0 = \hbar ck/2, \tag{7}$$

where E_0 is the zero-point energy of the oscillator [53, Chap. 5], $\hbar$ is the reduced Planck constant, and c is the speed of light. Alice's energy E_{i_n}, defines her state based on the boxes she set up in a GS, given her momentum transfer moving the prize to the other box as her TS. From this oscillator, a BEC can be achieved by quantifying energy E_0 [48, 61]. One can assume the prize energy state to be any m energy level of GS in a model step (a PDI), which is the non-zero energy in the oscillator. Bob can equivalently assume energy E_0 as his state, like anyone else who contributes to the system's total energy, i.e., all the information,

$$E = \overbrace{E_0(2mi_m + 1)}^{E_{i_m}\text{ energy levels}} + \overbrace{E_{i_1} + E_{i_2} + \cdots + E_{i_N}}^{\sum_n^N E_{i_n}}, \tag{8}$$

as the sum of all $(N+1)$-particle energies, i.e., E_{i_n} of N participants and E_{i_m} of the prize. To obtain the information, quantum field projections are required which involve the measurement of the uncertainty in E as ΔE discussed below.

Remark 8. A loop, or a series of GSM productions from a broad range of GSs, can scale to the production of BECs from a specific GS, Figs. 4 and 1(b), [38–41]. This occurs by trapping an atom in a lattice site as a strongly correlated system, Example 2. The produced BEC has a linear momentum near 0, and an inverse correlation to the moment it gains momentum $\gg 0$. This is by switching off the magnetic and laser fields from a light-atom interaction [1, 38, 54]. Here, the trap's lifetime has expired and the release of the GS particle to an ES is expected, Sec. 2.2. However, GSs separated from ES levels by an energy gap in a quantum oscillating trap [90], can be observed within a GSM regime projecting excited states of BEC in the trap for quantum information processing [7, Figs. 1–3].

The state of participant n, $|i_n\rangle$, can be read from E via a pairwise interaction with Bob as product $|ij\rangle = |i\rangle \otimes |j\rangle$. This tensor product represents space $\mathcal{S}$, and captures all the dynamics of particles that interact in $\mathcal{S}$, as described by their density matrix [94], and $\mathcal{T}(i)|i_m\rangle$ from Eqs. (1)–(1c). To find $\mathfrak{r}$, Bob can assume the crossover $|1_m\rangle \rightarrow i = 1$ from Eq. (1) via j, as $i_m \leq i_n$ in Eq. (6). Bob at step 5, can assume the lowest possible energy state as $m \rightarrow 1$ in Eq. (8) between two boxes, one with energy E_0, and the other with a photon energy (the prize) as $2E_0$. The change in energy, independent of a κ-based field transformation between energy states is

$$\Delta E = E_{i_n} - E_{i_m} = 2E_0|\Delta i|, \quad \text{and} \quad |\Delta i| = |i_m - i_n|, \tag{9}$$

which gives the possible expected outcomes of $\mathcal{S}$ as listed in Table 1, given i_m and i_n values to determine i. The following example discusses the energy eigenvalues, eigenstates and prediction outcomes in Table 1 via Eqs. (6)–(9).

Example 1. From Eq. (7), and by applying the single-field transform from Eq. (6), $E_1\Psi = 3E_0\Psi$ is returned in Bob's field, and $E_2\Phi = 5E_0\Phi$ is returned in Alice's field in superposition with the prize. The box in state $|1\rangle$ has a photon energy $2E_0 = \hbar ck$, if $\kappa^2\Psi E_1 = 3E_0\Phi$ is applied, according to $E_2\Phi - \kappa^2\Psi E_1 = 2E_0\Phi$. The key to predict the box with the prize as a *certain* outcome, is to calculate κ relative to the probability amplitude of Bob's field transforming into Alice's field as a QDF transformation. The top two rows of Table 1 show Alice, Eve and Bob interact toward model steps 4–6. The entanglement is when Alice's and Bob's fields correlate by measuring the QDF correlation function, as defined in Sec. 4.2. The third and fourth rows denote an entangled prize or no prize state with Bob or Alice, given $i_m = i_n$. The *ceratin* measurement outcomes can be satisfied by including Eve as the third party based on Eqs. (1b) and (1c) via $\mathcal{T}(i)$. The *uncertain* outcomes in Table 1 can be interpreted as a QPT, or a crossover to CPT for the prize hidden from Bob, as Alice's TS, while he decides or switch to attain his TS. For example, in the fifth row, a box with

Table 1
State prediction outcomes corresponding to events in QDF space $\mathcal{S}$. All outcomes are based on calculating κ and the field transformation between the system energy input and output. The κ-based field transformation occurs between Bob's field and other participants as listed under "photon." The photon projects state j onto Bob's field at his decision point (left two columns), and that state depending on i_m and i_n values, determines the outcome (from middle to right columns). An *uncertain* outcome is when the quantum information on the κ-based field transformation is not accessed by Bob, see [7], p. 16.

$\|i_m\rangle$ via $j \in \|ij\rangle \to \|i_m i_n\rangle$	State projected by photon	ΔE in GS/ES; $\|\Delta i\|$; i	Box prize state $\|i_m\rangle$ at step 4, 5, 6 or 7	κ-based outcome
$\|1\rangle$ via $\|12\rangle$	Eve via Alice	$2E_0$ in ES; 1; 1	box with prize; remaining box is 0 prize	certain
$\|0\rangle$ via $\|01\rangle$	Alice to Bob	$2E_0$ in ES; 1; 0	prize is suggested to Bob; Bob predicts 0	certain
$\|1\rangle$ via $\|11\rangle$	Eve via Alice	0; 0; $i_m = i_n = 1$	prize is entangled with Bob or Alice	certain
$\|0\rangle$ via $\|00\rangle$	Eve via Alice	0; 0; $i_m = i_n = 0$	0 prize is entangled with Bob or Alice	certain
$\|0\rangle$ via $\|02\rangle$	Alice or Audience	$4E_0$ in GS/ES; 2; —	prize is in superposition: poor or else	uncertain
$\|1\rangle$ via $\|10\rangle$	Alice or Audience	$2E_0$ from GS; 1; —	prize is hidden while Bob decides	uncertain

no prize is known to Bob as $i = 0$, while a box in state $|i_n\rangle \to |i\rangle = |2\rangle$ set up by Alice is in a superposition state.

The probability amplitude for finding the state of a particle interacting with Bob, is the inner product $\langle\phi_{i_n}|\psi_{i_n\to i}\rangle$, which can be evaluated within the thermodynamic limit. This evaluation is made by using the Born rule [47, 86], which connects the QDF game to the experiment [7]. The probability is the magnitude squared of the amplitude

$$\left|\langle\phi_{i_n}|\psi_{i_n\to i}\rangle\right|^2 = \left|\langle\phi_{i_n}|\psi_i\rangle\right|^2 /3n_d^2, \tag{10}$$

where $n_d \leq 2(N-1)/3$ is the number of particles interacting with Bob across distance $2d/3$ relative to $|\mathfrak{r}|$, set up by Alice. This number is comparable to the number density, where N is counted per unit volume $|\mathfrak{r}\mathbf{r}|^{3/2} \in \mathcal{S}$. As $\{|\mathfrak{r}\mathbf{r}|^{3/2}, N\}$ approaches ∞ for N interacting particles in superposition, a constant can be derived relative to n_d within the thermodynamic limit [80]. These interactions can result in Bob assuming state $|i_n\rangle \to i = 1$ via entanglement. This is discussed in Sec. 5 by predicting $\mathfrak{r}$ and evaluating κ via λ_c within the thermodynamic limit.

As presented in [7, Meth. Valid. I], and Sec. 2.2, photons, photoprobes and atoms within their interacting fields are like suits that the game participants can change relative to a scalar field (QDF) measurement made in a QDF circuit. The Refs. [25, 69] followed by the method to implement the QDF algorithm, are given in [7, 9].

Sections 4.2–6.3, present the statistical system as a set of game participants relative to the prize, which has one or more PTs. To constitute a thermodynamic system, Eq. (10), the number of particles should be of the order of the Avogadro's number. Here, $\mathcal{S}$ in Fig. 1, denoting the QDF game room in Fig. 6, gets full by one or more rounds of the model steps, Sec. 2. However, every member of the system, Bob, Alice, etc. is also considered as a thermodynamic system that may have a PT as the thermodynamic system of one particle attaining a TS. This removes the queuing of particles in populating different TS's when one or more participants attain them in that queue. This is when the QDF system evolves over time by registering and counting qubits that denote a set of TS's attained by one or more participants (step 8), [7, Meth. Valid. II]. Hence, the possibility of exceeding the qubit memory limit, i.e., the sum of step 8 readouts in Fig. 1(a), is removed over time, which is the sum of repeated TS's subtracted from the step 8 sum. In a series of repeated TS's, the system can reach near zero entropy or no information satisfying a deterministic picture (see [7, pp. 11-13, 29] in predicting BEC EPR pairs and a TS). Bob in his GS state is a BEC that can turn into a non-BEC exited atom (ES) as his TS via interaction with a photon from Alice's or someone else's field, as referenced and exemplified in Secs. 4.2.2, 5.1, and [7, Meth. Valid. I]. The mathematical proof to win the prize is presented in Secs. 7 and 8.

4.2. QDF transform via particle pairing

4.2.1. Particle pairing

Given the *doubling metric spaces* concept [2, 3], the QDF transform is defined as follows.

Definition. A scalar QDF is a field where its spatial dimensions are doubled by a pairwise field scalar operation. This operation collapses the field to its pair with an ST probability of $\mathcal{P}(\Psi \leftrightarrow \Phi) = |\langle\Psi\Phi\rangle|^2 \ni \langle\mathbf{kr}\rangle$, where $\langle\Psi\Phi\rangle$ is the QDF correlation function. The field dimensions cancel out in this function, if via κ, $\mathbf{k}$ and $\mathbf{r}$ correlate from Eq. (2).

This is satisfied as $|\mathbf{kr}| \to 1$ from Eq. (17) over a lifetime correlation t_c between two field points a and b of distance $d(a,b) \propto \lambda_c(\lambda_c \to ct_c)$, where a PT occurs.

The QDF definition and its metric space are illustrated in Fig. 2, corresponding to Figs. 1 and 6 events. These events occur within the QDF, given the energy input E_{in} and the energy output E_{out}. The middle (*switch*) section of Fig. 2, corresponding to the switch in Fig. 1 or 5, focuses on the field dynamics contributing to a QDF transformation. This projects data from the quantum metric space to the area of pairwise interactions $|\mathbf{r}\mathfrak{r}|$, Sec. 4.1. As a result, the QDF system dynamics are state superposition, entanglement and teleportation. The QDF transform denotes the expected measurement outcome of Bob's decision, which is the probability measure shown at the switch. The outcome of Fig. 2 right correlates to the fmv of the switch dynamics.

In Fig. 2, from left-to-right, a quantum field or a PT, is described by a set of wavefunctions

$$\mathbb{F} = \left\{\Psi, \Phi, \Psi^2, \Phi^2, \Psi\Phi, \Phi\Psi, \ldots\right\}, \tag{11}$$

where a set element $\ell \in \mathbb{F}$ is dimensionless or else, e.g., see Refs. [21, 70, 71]. The field has a radius of R that maps to the sum of the subfield radii. The subfield radii ≥ 2 field positions can be occupied by n_d particles, Eq. (10), with probability $\mathcal{P}$ between their positions of $\mathbf{r}_{i,j}$ in $R \subset \mathcal{S}_{\mathbf{r}}$. Each subfield pair is occupied by an interacting particle pair on the input side as a pairwise particle position. The number of pairwise particle interactions is

$$\mu_{ij} = (N^2 - N)/2. \tag{12}$$

From Eqs. (2)–(6), the momentum transfer from a particle to its pair with lower energy can result in a PT. This is described in Fig. 2 through the switch function $\langle f(\kappa)\mathcal{T}(\mathbf{r})|\mathbf{k}\rangle$, which satisfies a field transform moment derived from the reciprocal as $\kappa\Phi \to \kappa^{-2}\Phi\ell R/2 = \Psi\ell d(a,b)$. The momentum transfer causing a PT is expressed by

$$[\mathbf{k}_{i,j}^2]^{1/2} < \lambda_{\text{P}}^{-1}, \qquad |\langle f(\kappa)\ell\rangle|\lambda_{\text{P}}^{-1} \to \infty, \tag{13}$$

[63, 76, 77], where the information is shared as energy partitions between the pair via projection in e.g. a spin-lattice model [7, 55], and $|\langle f(\kappa)\ell\rangle|$ denotes the expected PT, so that $[\mathbf{k}_{i,j}^2]^{1/2} < \lambda_{\text{P}}^{-1}$. For this PT, a photon and an atom increase the amount of information within their field of interaction as a pair, to the point where the field doubles in its finite metric space. This is exemplified in the creation of BEC EPR pairs below, or see [7, Example 2B].

4.2.2. The QDF transform

The next three examples followed by Eqs. (14)–(20), describe the QDF transform. In these examples, experimentally, Bob is a BEC when entangled with the prize state within the GS regime (a series production of different GSs, Fig. 1(b)). The prize is a BEC if it comes from a series of GSM productions by Alice as a BEC [39–41]. Conversely, Bob is a cold atom, else an excited atom when from a trap (box) the prize once entangled with Bob is released with an equivalent amount of energy relative to its mass (see energy operators in [7]). This is observed through superdense coding, where classical bits of information are decoded by sharing the entangled state after teleportation [7].

From the QDF definition and [7, 56, 57], a BEC EPR production, entanglement and teleportation can be modelled within a correlated system of traps. This is by using a laser beam splitter which operates on a BEC prepared in a spin coherent state [56]. The spin is rotated to a maximally polarized spin, and thereby squeezed by one-axis twisting to create entanglement between BECs [56]. In our proposed method [7], the squeezed BEC spin is produced from an area of traps in a spin-lattice model. A BEC is split into two from an area of particle interaction with the beam. A spin-spin operation is applied to the two BECs, and get them entangled. This satisfies a continuous transformation of $\mathbf{k}_{i,j}|\mathbf{r}| \to |\mathbf{kr}| \to 1$ between the entangled EPR pair where teleportation is conducted, according to Eq. (16).

Example 2. In the deterministic picture, a BEC EPR pair is produced and entangled with Bell correlations between their observables [56]. Alice and the prize in a box, as a pair, like in Eq. (1c), can represent the sum of Bell correlations from the four possible combinations of Bell states

$$|ij\rangle_{\substack{\text{Alice}\\ \text{prize}\in\text{Box}}} = |\{00, 01, 10, 11\}\rangle_{\substack{\text{Alice}\\ \text{prize}\in\text{Box}}}.$$

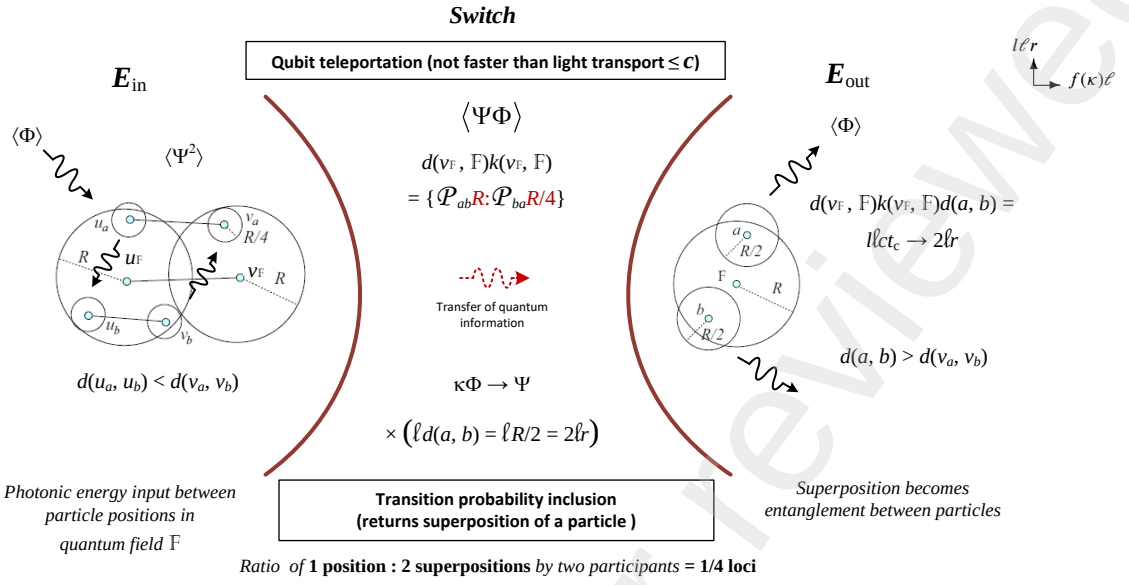

Fig. 2: The QDF metric space. The dynamics of particle interactions are mapped to QDF model steps in Figs. 1 and 6. (Left side) Photon energy is exchanged between a photon (Alice) and an atom (Bob), and a quantum particle (the prize) at field positions, u_a and u_b, as $\mathbf{r}_{i,j}$, Eq. (3). The spatial dimensions double between the two positions, $u_a \to u_b$ and $v_b \to v_a$, due to the quantum particle's behaviour resulting in its superposition, Eq. (1). This forms central field points $u_{\mathbb{F}}$ and $v_{\mathbb{F}}$, where superposition and entanglement occurs between the interacting particles. (Middle) This is where quantum information can be transferred via qubit teleportation at the switch with some probability, Eq. (15), measured between the energy input side and the energy output side. Particle momentum $k(v_{\mathbb{F}}, \mathbb{F}) = |\mathbf{k}| = k$ from Eqs. (17)–(20), is measured between the four probable positions, all of which their observable energy states can be superposed by two particles or a combination of two photons and a particle (Alice, an audience member and Eve). If one of these particles transfers the quantum information to the atom (Bob), given $k^2 = 1$, Eq. (17), the atom for its TS can entangle its state with the targeted quantum particle (the prize). (Right side) Superposition leads to entanglement since the quantum information of the atom has doubled at the switch when the QKD from the source is projected onto the atom's space [7, pp. 4–12]. This is the space where Eve or an audience member share the quantum information with Bob, thus doubling the probability of one of the field positions, a or b, to be the prize. The latter is revealed when quantum decoherence occurs from the release of a photon energy from the prize relative to the total energy release from Bob and $N-1$ participants.

The BEC EPR pair can perform a quantum teleportation [57] e.g., Alice at a laser beam splitter is the sender of the qubit information on the prize state to a box as the receiver. The box with the prize can teleport its state to another box while being entangled with Alice. The teleportation protocol is presented in [7, Example 2.B]. The prize state remains entangled with Alice. However, the prize becomes a GSM or a BEC in one of the boxes, after the box performs a phase-space displacement on its GS mode (half of the EPR pair), to recover the original unknown input state from Alice, and change or unchange the prize state. If changed, the BEC in the box can split into two BECs entangled between two boxes, each with a prize state [7, Eq. (17)]. The QDF is formed between any of the traps and Alice, establishing a distance of $d(|\mathbf{r}_i|, |\mathbf{r}|) = \langle R/2 \rangle = 2|\mathbf{r}|$ from Eqs. (14)–(30), Fig. 2. The symmetric property of the positions can be observed from the interaction area $|\mathbf{r}\,\mathbf{r}|$ of the entangled pair. An entangled EPR state has perfect correlations [57] in the pair's position and momentum, which have the variances

$$\Delta\left(\mathbf{k}_{i,j}\right)_{|\mathbf{r}\,\mathbf{r}|} \to 0 \quad \text{and} \quad \Delta\left(\mathbf{r}_{i_{|\mathbf{r}\,\mathbf{r}|}} + \mathbf{r}_{j_{|\mathbf{r}\,\mathbf{r}|}}\right) \to 0,$$

respectively, satisfying the deterministic picture [7, 57]. The entangled Hamiltonian of the QDF between the traps is presented in [7, Eq. (17)]. The deterministic picture evolves into a probabilistic picture, Sec. 2.2, which predicts classical bits form the BEC EPR state (Bell states) as the qubit information shared between game participants. This is

denoted as superdense coding which is the inverse of teleportation, as implemented in the QDF circuit [7].

Example 3. From Sec. 2.2.2, Example 1 and Eq. (13), consider Eve via Alice's field superposing between the pairwise field positions. Also, consider a photon from Alice's field (or audience, Table 1 bottom two rows) paired with an atom Bob, as in Example 2. Then, say, within the ΔE-limit from Eq. (9), the photon shares 8 parts of its quantum information (a pump laser as a source of photons [62], or Fig. 1(a) to 1(b)) about $|\mathfrak{r}|$ with the BEC atom Bob through beam interaction. This information denotes the amount of pumped photons interacting with the atom that emit pairs of entangled photons whose internal polarization states are entangled light modes from the QDF of the BEC EPR pair. The pair, in return, with a third party Eve, shares 9 parts within the laser-driven field of all particles. Potentially, the pair has 8 parts predicted, and the photon has 1/2 of the EPR state observed after qubit scattering, Fig. 1(b) to 1(a). This qubit is prepared by Eve in the ES, and scattered by the two GS traps which are produced by two target qubits from a beam splitter operation by Alice, which created the EPR pair in a fixed GS, [7, Example 2], Eq. (1c). This is 1 part of the quantum information on the prize position $|\langle \mathbf{r}\mathfrak{r}\rangle|^{1/2}$ scattered off as entangled photons with a factor of $e^{\imath\mathbf{k}(\mathfrak{r}-\mathbf{r})}$ in Eq. (38). However, if two emitted photons are entangled from the shared BEC EPR source via Eve (an extra qubit to entangle) [62] (Table 1 fourth and sixth rows), then both have 9 parts of the information ε, where $\varepsilon \leq 1$. Thus, the photoprobe has 9 parts of quantum information if it constantly reads $\mathbf{k}_{i,j}\mathbf{r}$ relative to R as it propagates, $\phi_{i_n}(\mathbf{k})e^{\imath\mathbf{kr}}$ in Eq. (6). These particles carry each other's quantum information (Bell states) [10, 37], as $\varepsilon \in [8/9, 1]$ between $l \geq 4$ field positions, doubling their field radii with a probability ratio of $\varepsilon : l$ (loci), Fig. 2. A value of $\varepsilon = 1$ denotes no more quantum information of the prize state is exchanged, or zero entropy. The scattering as a no prize state in the QDF circuit is presented via Eqs. (31)–(38).

Example 4. From Eq. (12), there are μ_{ij} pairwise interactions in a QDF for either field transformation $\Psi(\mathbf{r}) \to \Phi(\mathbf{k})$ or $\Phi(\mathbf{k}) \to \Psi(\mathbf{r})$ in Eq. (6). These interactions for Example 3 events, results in 6 positions: 2 photonic superpositions projected from Alice at the beam splitter onto an atom's space with two positions where photoprobe Eve observes, and 2 atomic positions from the atom after it splits as a BEC EPR pair. The ratio of occupying positions in carrying the quantum information by the EPR pair via the beam splitter interaction [33, 56], is $8 : 9$. In total, with the entangled EPR state, there are $6 + 2 = 8$ parts of quantum information shared with an extra entangled qubit provided by Eve. This returns a ratio of $8 : 9$ parts of information exchanged between particles. Figure 4 shows where a laser beam as the light source contributes to a BEC production [25, 64] and the pairwise positions of entangled pairs in a QPT.

Given the least uncertainty in Eqs. (2) and (5), and $\min l = 4$ from Example 3, the quantum information exchange with some probability $\mathcal{P}$ between two field points, a and b, is

$$\min lr\mathcal{P}_{ab}/2\mathcal{P}_{ba} \xrightarrow[\text{switch}]{\kappa\text{-field}} 4\mathbf{r}_{i,j}|\langle f(\kappa)\ell\rangle| = \langle R/2\rangle, \tag{14}$$

where $r = |\mathbf{r}|$, and $\{\mathcal{P}_{ab}/\mathcal{P}_{ba}\} \to |\langle f(\kappa)\ell\rangle|$ describes a PT into a QPT or CPT as it decays over time t_c.

In Eq. (14), r is a subfield radius as the distance between the information source and Bob's position. The transformation also denotes a PT caused by particle interactions at the switch. The quantum information transfer occurs at the switch via qubit teleportation [25, 57]. This is determined by taking the difference between two probability ratios of the superposing particles output state (Fig. 2 right side) as the prize to be in one of the two field positions, which is

$$\Delta\mathcal{P} = \left|\mathcal{P}_{ab}R - R\mathcal{P}_{ba}/4\right|. \tag{15}$$

Given the particle information exchange as a qubit teleportation [31], and $\langle \mathbf{kr}\rangle_c$ with the least uncertainty, the information transfer rate via $f(\kappa)$ between a particle pair of two field points is

$$\frac{d(a,b)}{t_c} = \frac{\mathbf{r}_{i,j}}{t_c}\left|\langle \mathbf{kr}\rangle_c\right| \xrightarrow[\text{switch}]{\kappa\text{-field}} \lim_{|\mathbf{kr}|\to 1}|\langle \mathbf{kr}\rangle|\frac{r}{2t_c} \leq c. \tag{16}$$

The subfield radii on the energy input side is expected to double on the energy output side. This is due to quantum superposition of Bell states becomes entanglement between the particle pair [31], e.g., entanglement between Bob and

the prize over their lifetime correlation t_c of their states.

Remark 9. The lifetime of a state, t_c in Eq. (16), has the imaginary part of a QDF transformation, which denotes the *imaginary interaction* part of a particle pair's energy. The moment of this interaction is determined by calculating the double-field scattering amplitude [93] from a photon scattering field, as discussed in Sec. 6 field intensity products.

5. QDF circuit and state prediction

Particle states can be predicted through a scalar field switch and the relevant PDI choice to measure the fmv from Sec. 3. An entanglement setup by a quantum circuit in Sec. 5.3, and its QDF thermodynamics via κ in Secs. 5.2 and 6, gives a strong prediction in the QDF model, in theory and its application, Sec. 7.

5.1. QDF switch and phase transition

From the QDF definition and Eqs. (2)–(6), (10), (16), the ST probability of a QDF for an expected particle's TS is

$$\mathcal{P}(\Psi \leftrightarrow \Phi) = |\langle \Psi\Phi \rangle|^2 \propto |\langle \Psi(\lambda_P)|\Phi(\lambda_c^{-1})\rangle|^2 \geq 1/2, \tag{17}$$

where $|\langle \Psi\Phi \rangle|^2 \geq 1/2$, if field component $\mathbf{k}$ or $\mathbf{r}$ is multiplied by κ satisfying a scalar convergence of $|\mathbf{kr}| \to k^2 = 1$. From this convergence and an expected superposition between a particle pair $|\langle \Psi|\mathbf{kr}|\Phi\rangle| = 1/2$ in Eq. (5), the constant of inverse or direct variation can be derived

$$|\langle \Psi\Phi \rangle|^2 \left| \sum_{\dot{l}=1}^{\mu_{ij}} \langle \mathbf{kr} \rangle_{c_{\dot{l}}} \left\langle \Psi(\lambda_P)|\mathbf{kr}|\Phi(\lambda_c^{-1}) \right\rangle \right|^{\pm 2} \to k^2 = 1, \tag{18}$$

where the sum is the correlations sum between pairwise states. The sum satisfies the maximum ST probability, $\max \mathcal{P}(\Psi \leftrightarrow \Phi) = 1$ for $\dot{l} \in [l-3, \mu_{ij}]$ pairwise interactions relative to t_c from Eq. (14). The sum approaches 2, as $|\langle \Psi\Phi \rangle|^2 \to 1/2$ varies directly with $|\langle \Psi|\mathbf{kr}|\Phi\rangle|^2 \to 1/2$ in Eq. (17) for a particle pair in superposition, where μ_{ij}-minimum is $\min \mu_{ij} \to 1$. The sum tends to 1, as $|\langle \Psi\Phi \rangle|^2 \to 1/2$ varies inversely with $|\langle \Psi|\mathbf{kr}|\Phi\rangle|^{-2} \to 2$.

Any correlations sum > 2 in Eq. (18) satisfying $\max \mathcal{P}(\Psi \leftrightarrow \Phi)$, denotes a Bell state, Sec. 5.3. An inverse correlation between field components in Eq. (18) is expected under the κ-based field transformation, as $|\mathbf{k}| = 2\pi\lambda_c^{-1} \to \infty$, $|\mathbf{r}|$ tends to λ_P, where $\lambda_c \to \lambda_P$ [63, 76, 77]. This denotes a photoprobe observes a photon travelling across a distance of $2|\langle f(\kappa)\ell \rangle|r \to \lambda_P$ between two field points, Eqs. (14)–(16), relative to its interaction with a quantum particle in a GS at distance $|\mathbf{r}| \to \lambda_P$. The prize frequency can be measured from its position somewhere at $d \in [2|\langle f(\kappa)\ell \rangle|r, \lambda_c]$, Figs. 3–5. This information comes from two correlations, one being inverse to the other, and can be obtained from the photoprobe as the prize state projected onto the atom's space. From Example 3, Eve via Alice as a photoprobe shares Alice's TS with atom Bob and returns an inverse correlation to Bob's TS, if there is only one prize to win (step 8).

As illustrated in Figs. 1–5, photons contribute to field emissions in a PT that cause a switch. In the switching process, the expected energy output is lower than the energy input, $\langle E_{out} \rangle < E_{in}$, where $\langle E_{out} \rangle$ is *useful* [43, 44] to Bob if he wins the prize as his TS. This can be interpreted as a momentum transfer from the prize to Bob relative to E_{in} coming from $N-1$ participants. An example of transferring energy input to useful energy output is to construct an efficient (useful) quantum computer. In this computer, switches are used to conduct operations on qubits described by e.g., the Hamiltonian acting on qubit pairs [7, 44].

Model steps 3–6 focus on Bob exchanging energy with participants to decide (cause a switch or not switch) which box is with the prize in step 7? Thus, $\langle E_{out} \rangle$ can be predicted as the change $\Delta E\ell$ from Eq. (9) is measured

$$\overbrace{\langle \Psi|E_{in}|\Phi\rangle}^{\text{input}} \longrightarrow \overbrace{|E_{i_n}\langle \Psi|\Phi\rangle|}^{\text{switch}} \longrightarrow \overbrace{|\langle f(\kappa)\Delta E\ell \rangle|}^{\text{phase transition}} = \overbrace{\langle E_{out} \rangle}^{\text{output}}, \tag{19}$$

where the switching operation via $f(\kappa)$ is between energy states, Eqs. (6)–(9). The use of $f(\kappa)$ is in predicting particle states and a PT via κ, and denotes the interaction of a pair of particle fields resulting in a PT, Sec. 5.3.

The correlation between the output, the switch, and the input in Eq. (19) is determined by measuring the ST probability of the field transformation. This measurement is from a distance between two field points,

$$\lim_{|\mathbf{kr}|\to 1} d(a,b)\ell|\mathbf{kr}| = d(\upsilon_{\mathbb{F}},\mathbb{F})k(\upsilon_{\mathbb{F}},\mathbb{F})d(a,b) \longrightarrow d(a,b)\ell = \ell R/2 = 2\ell r \leq l\ell ct_{\mathrm{c}}, \tag{20}$$

where a PT decays over time t_{c} with some probability, Eq. (14), as $ct_{\mathrm{c}} \to \lambda_{\mathrm{c}}$ after a κ operation, and $d(\upsilon_{\mathbb{F}}, \mathbb{F})k(\upsilon_{\mathbb{F}},\mathbb{F}) = |\mathbf{kr}|$ from Eq. (18). This measure is required to determine the state and position of the prize relative to any other quantum particle interaction during the scalar field operation. A quantity of $l\ell ct_{\mathrm{c}} \to l\ell\lambda_{\mathrm{c}}$ relates to the correlations sum in Eq. (18), which satisfies $\max \mathcal{P}(\Psi \leftrightarrow \Phi)$ in Eq. (17).

In Eq. (14), an output state projection from Φ onto the input state from Ψ via $f(\kappa)\ell$ gives a photoprobe a linear superposition and a $\mathcal{P}(\Psi \leftrightarrow \Phi) \geq 1/2$ of a QDF. From Examples 3–5, there are 6 positions in a QDF for $\min \mu_{ij} = 3$ pairwise interactions: 2 photonic superpositions from Alice and Eve, and 2 atomic positions from Bob entangled with the prize or with a prize (as one of the entangled BEC pair produced by splitting a BEC via Alice).

A pairwise interaction over superposition $\psi_{ij}(\mathbf{r}_{i,j})\,|ij\rangle$, has a QDF projection product

$$\mathbf{P}_{\Phi\Psi} = \mathbf{P}_{\Phi}|\psi_{ij}\rangle = |\phi_{i_n}\rangle\langle\phi_{i_n}|\mathcal{O}|\psi_{ij}\rangle, \tag{21}$$

where $\mathbf{P}_{\Phi}$ is the projection operator, $\mathcal{O}$ is the $\mathbf{kr}$ operator as an observable after measurement (by Bob, Alice or Eve), and $\mathbf{P}_{\Phi\Psi}$ denotes transforming $|\psi_{ij}\rangle$ of positions in field Ψ into $|\phi_{i_n}\rangle$ of momentum in field Φ, Eq. (6). The superposed states $|\psi_i\rangle$ and $|\psi_j\rangle$ as $|\psi_{ij}\rangle$, project in the direction of $|\phi_{i_n}\rangle$ which can lead to entanglement between a particle pair [28], as in entangled Bell states [31]. As states $|i\rangle$, $|i_n\rangle$ and $|j\rangle$ correlate from the correlation function $\langle\Psi\Phi\rangle$, Bob can use the information on the product state $|ij\rangle = |i_n \to i\rangle \otimes |j\rangle$ to predict i, to either switch, to attain his TS, see Eq. (9).

In Eq. (18), $\min \mu_{ij} = 3$, applies to a pair of particles interacting with the prize in steps 6 and 7. A third participant gathers information about the prize and shares it with Bob. The sum of all particle interactions is counted by their $\mathcal{O}$ with a degree of quantum variance. This determines the energy change of a particle relative to the prize by

$$\mathcal{O} = [\mu_{ij}/\min \mu_{ij}]^{1/2}\delta^{-1/4} \geq 2, \text{ given } \delta = \left|\Delta\mathbf{r}_{i,j}^2\mathbf{k}_{i,j}^2\right| \in (0,1], \tag{22}$$

where $N > 3$ satisfies $\mu_{ij} \geq 6$ interactions of all participants relative to $\min \mu_{ij} = 3$ interactions of three participants, and $\Delta\mathbf{r}_{i,j}^2 = \mathbf{r}_{i,j}^2 - |\mathbf{r}|^2$ is the *quantum state separation* from the photoprobe momenta $\mathbf{k}_{i,j}^2$, denoted by δ. The extent of this separation is determined with a variance degree of $\delta^{-1/4}$. The farther $\mathbf{r}_{i,j}$ is from λ_{P} denoting a quantum state, the greater λ_{c} is to determine i of the prize (Sec. 5.2).

The inequality of Eq. (22) can be evaluated by plugging in the relevant variable minima and maxima. For $|\langle\Psi|\Phi\rangle| = |\langle\Phi|\Psi\rangle| = 0$, $|\Psi\rangle$ and $|\Phi\rangle$ are orthogonal, and $\mathcal{O} = 2$. The decomposition of each field function would have a combination of orthogonal and nonorthogonal states [18, 74] as quasi-Bell states, Eq. (1b), where one or two pairs of states are indistinguishable [7, Eqs. (24)–(26)]. As a result, pairs of information bits are hidden and cannot be discovered unless the field is complemented by an external field from the QDF. This is an extra qubit provided by one of the two fields of the QDF, as Eve's state which complements the nonorthogonality of two or more participants paired with the prize state. This yields orthogonal states as pure and separable in $\mathcal{S}$, and denotes decoherence without entanglement as a known model step outcome in Table 1, see Remark 5. Prior to decoherence at the switch, as $|\langle\Psi|\Phi\rangle| \to 1$, $|\Psi\rangle$ is the same quantum state as $|\Phi\rangle$ under $\kappa^2\Psi \to \Phi$ from Eq. (6).

In Eq. (10), the probability that the system is in state $|\psi_{i_n}\rangle$, can be measured from the norm relative to $\mathfrak{r}$ from state $|\psi_i\rangle$, such that a continuous transformation $\mathbf{k}_{i,j}|\mathbf{r}| \to |\mathbf{kr}| \to 1$ returns a constant in Eqs. (6) and (18) for $\max \mathcal{P}(\Psi \leftrightarrow \Phi) = 1$. However, given the minima, $N \to \min f(N) = 4$ for μ_{ij}, 3 for $\min \mu_{ij}$, and $\mathbf{k}_{i,j} \to \min \mathbf{k}_{i,j} = |\langle\Phi|\mathbf{kr}|\Psi\rangle|/2\mathbf{r}_{i,j} > 0$ from Eq. (5), the maxima of $\mathcal{O}$ fall in the open interval

$$\max \mathcal{O} = [2\mu_{ij}/3]^{1/2}\left|1 - 4\mathbf{k}_{i,j}\mathbf{r}\right|^{-1/4} \in (2,\infty). \tag{23}$$

The significance of measuring $\mathcal{O}$ is when its values relate to the correlations sum in Eq. (18).

Example 5. Two particle pairs of $\min f(N) = 4$ in superposition interact relative to the prize with a factor of uncertainty $|\langle\Phi|\mathbf{kr}|\Psi\rangle| = 1/2$, Eq. (5). A third particle, Eve, transfers the prize state to one of them, according to Eqs.

(1b)–(6). This gives $\mathcal{O} = 2\sqrt{2}/3^{1/4} \approx 2.1$, which tends to quantum decoherence without entanglement, according to Eqs. (21)–(23). However, the numerator alone denotes the prize is entangled with a particle pair.

5.2. Scalar κ

Classical state i is determined by measuring how far a particle is from a PT, which is the difference between λ_c for a particle pair and their interaction distance

$$|\Delta d| = |d - \lambda_c/4|, \qquad d \xrightarrow{|\Delta d|} |\mathfrak{r}|. \tag{24}$$

Entanglement is determined if Eve observes a sate transfer between boxes (teleportation), Sec. 4.2, as she intercepts and shares information about $\mathfrak{r}$ on an entangled EPR pair with Bob (step 6). A BEC is revealed as $|\Delta d| \to 0$, denoting the no prize state or $i = 0$, else a prize state as a GSM or an ES particle (step 7), see Examples 2 and 3.

From the particle pairing concept, Sec. 4.2, and Eqs. (5), (22)–(24), a κ-based log relation can be deduced

$$\log_\kappa 2|\Delta d| = 2|\mathbf{r}| \overset{\mu_{ij}}{\longleftrightarrow} 2|\mathfrak{r}|\mathbf{r}_{i,j}\mathbf{k}_{i,j} \le n_d|\mathbf{r}|/\mathcal{O}^2, \tag{25}$$

and scalar κ has a field switch function using Eqs. (10)–(25),

$$|\langle f(\kappa)\ell\rangle| = \kappa^{2\cancel{|\mathbf{r}|}/f(N)\le n_d\cancel{|\mathbf{r}|}/\mathcal{O}^2} = \kappa^{N\max n_d/\mathcal{O}^2 \to 2} = 2|\Delta d|, \tag{26}$$

where $2|\Delta d|$ denotes a pairwise particle field interaction resulting in a PT, and $\max n_d = 2(N-1)/3$ from Eq. (10). The switch function $f(\kappa)$ links two input states observed from an interacting particle pair to an output state. A scalar order of κ^2 links all bounds of μ_{ij} interactions to the output state. A PT is expected for a TS, given that $N \max n_d = 4\mu_{ij}/3$ relative to $\mathcal{O}^2$ is observed when the superposition condition from Example 5 is applied to Eq. (23).

Second order PTs [79] on a scale of κ^4 can occur from the pairwise input states linked to the output state as

$$2|\kappa^4\langle \mathbf{r}\mathfrak{r}\rangle|^{1/2} = 2|\mathfrak{r}|\kappa^2 \overset{\mu_{ij}}{\longleftrightarrow} 4|\mathbf{r}\Delta d| = |4\mathbf{r}\mathfrak{r} - \mathbf{r}\lambda_c|. \tag{27}$$

Relative to $\mathfrak{r}$ on the output side of the equation, the form $4|\mathbf{r}|$ on the input side is derived. This creates a field with radius R having two subfields, each with radius $R/2$, as in Eq. (14). This is the expected outcome denoting particle superposition. For Bob's TS, if $\mathfrak{r}$ is measured from the $\mathbf{kr}$-field between Alice and the prize, κ in $f(\kappa)$ is set to a $\mathbf{k}$-dependent field Φ multiplied by Ψ, collapsing Φ of Alice to Ψ of the prize. For Alice's or Eve's TS, if the particle momentum is measured, the converse applies. From Eqs. (17) and (18), field switch operation is

$$f(\kappa)|\langle\Psi(\lambda_P)|\Phi(\lambda_c^{-1})\rangle|^{\pm 2} \in (0, 2], \tag{28}$$

where the $\pm$ sign denotes a field collapse to another via $f(\kappa)$, and the interval $(0, 2]$ defines the lower and upper bounds of κ, as discussed in Sec. 6. From Eqs. (13), (22)–(28), the photoprobe momentum transfer to its pair, which can result in a PT (or a switch), can be linked to the scalar by

$$\min \mu_{ij}[\mathbf{k}_{i,j}^2]^{1/2} = \lambda_c|\kappa|^{-4}. \tag{29}$$

This denotes the information on Bob's state is collected by the photoprobe at steps 5 and 7, and can be observed at a distance relative to Bob's position as $|\mathbf{r}| \to \lambda_P$. The scalar from Eqs. (26)–(29) for λ_c returns

$$\lambda_c = \min \mu_{ij} 4|\Delta d|^2/\sqrt{dr} \le \infty. \tag{30}$$

In this equation, for any $\mu_{i,j}$, as $d \to 1$, λ_c tends to $4d$ relative to $r \approx \lambda_P$, which denotes a PT expected between four possible positions in S. For $\lambda_c \gtrsim 2d$, as r and d tend to 1, λ_c diverges to ∞ beyond its lifetime correlation t_c. Any approximation of $\lambda_c^{-1}|\kappa^4| \approx \lambda_P$ as $d \to 0$ denotes a GS (no prize) or $i = 0$. A symmetry of $i = 1$ can provide Bob the information on $\mathfrak{r}$, which is $2|\mathbf{r}| \to |\mathfrak{r}|$ from Eq. (25) with the least uncertainty, Eq. (5). This is discussed next.

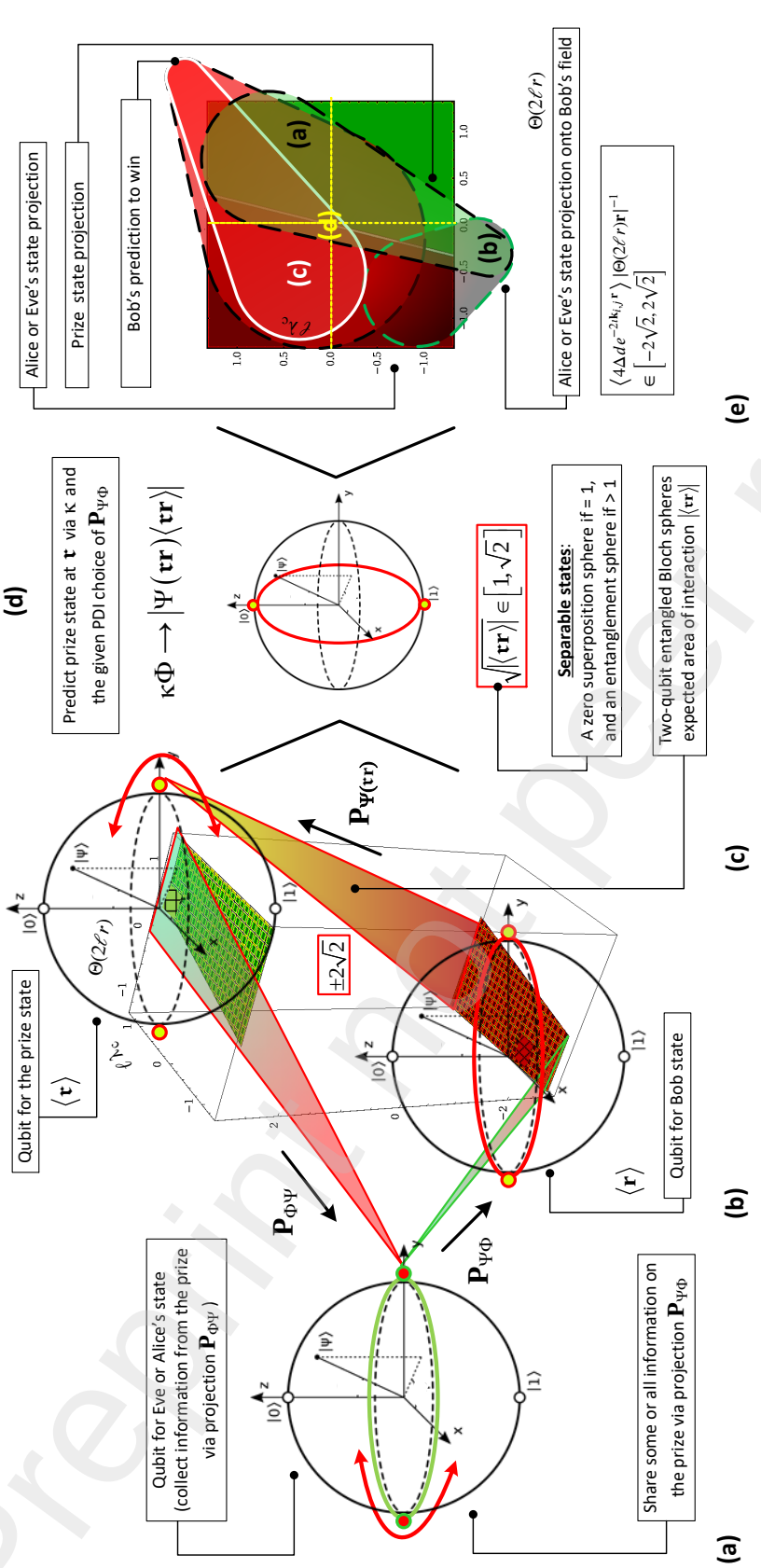

Fig. 3. PDI choice via projections $\mathbf{P}_{\Psi\Phi}$ and $\mathbf{P}_{\Phi\Psi}$ to determine $\mathbf{r}$ between a particle pair. **(a)** A qubit Bloch sphere representation of Eve or Alice's state that changes via projection $\mathbf{P}_{\Phi\Psi}$ of the prize state in the direction of a definite position. The qubit rotation around the z-axis denotes superposition (Bell state) between this qubit and the qubit representing the prize state in **(b)**. **(b)** Geometric representation of Eqs. (31)–(34) outcomes using two-qubit Bloch spheres. The spheres are entangled via projection from Bob onto the expected prize position $\langle \mathbf{r} \rangle$. From **(a)**, some or all the information about $\mathbf{r}$ is shared with Bob via projection $\mathbf{P}_{\Psi\Phi}$. **(c)** As the information grows and doubles in Bob's sphere via $\mathbf{P}_{\Phi\Psi}$, so does the value of $2|\langle \mathbf{rr} \rangle|^{1/2}$ given $d \in [0, 1]$ and $\lambda_c \rightarrow 1$ in Δd, Eq. (34). The result is $\pm 2\sqrt{2}$ for the min and max $2|\langle \mathbf{rr} \rangle|^{1/2}$ in the given projector's $\pm$ direction around the z-axis via $\mathbf{P}_{\Psi\Phi}$. This denotes entangled Bell states between the prize and Bob. A value of $\pm 2|\langle \mathbf{rr} \rangle|^{1/2} \rightarrow 0$ denotes two spheres meet at position 0 where classical state i is revealed. The two-qubit entangled spheres are projected via projections $\mathbf{P}_{\Psi\Phi}$ and $\mathbf{P}_{\Psi\Phi} \rightarrow \mathbf{P}_{\Psi(\mathbf{rr})}$, Eq. (39). The latter occurs in the expected area of interaction $|\langle \mathbf{rr} \rangle|$ between Bob and the prize, Eq. (27), where $|\langle \mathbf{rr} \rangle|^{1/2} \in [1, \sqrt{2}]$. **(d)** Zero superposition (separable states) is when $\mathbf{r}$ is predicted as $|\langle \mathbf{rr} \rangle|^{1/2} \rightarrow 1$. From $\langle \mathbf{r}|\psi_i \rangle$, other possibilities of a prize, no prize and the prize game outcome for Bob as one of the values can be expected from the rotation around the y-axis. **(e)** A cross-section of **(a)**–**(c)** complex and real sphere projections between Alice (Eve), Bob and the prize state. Here, the information is exchanged and grows for a strong predication relative to the temporal measure of Θ between pairwise field points. The information growth is shown in the **(c)**'s outer section, mutually intersecting with **(b)**, which leads to a strong prediction of possible prize states, as shown in the **(c)**'s inner section. The outcome of this prediction falls under area **(d)**, which separates Bob from the prize state as quantum decoherence or classical state i, Sec. 2.2. The fraction at the bottom is the expected pairwise interactions relative to the magnitude of their temporal correlation from Eq. (34).

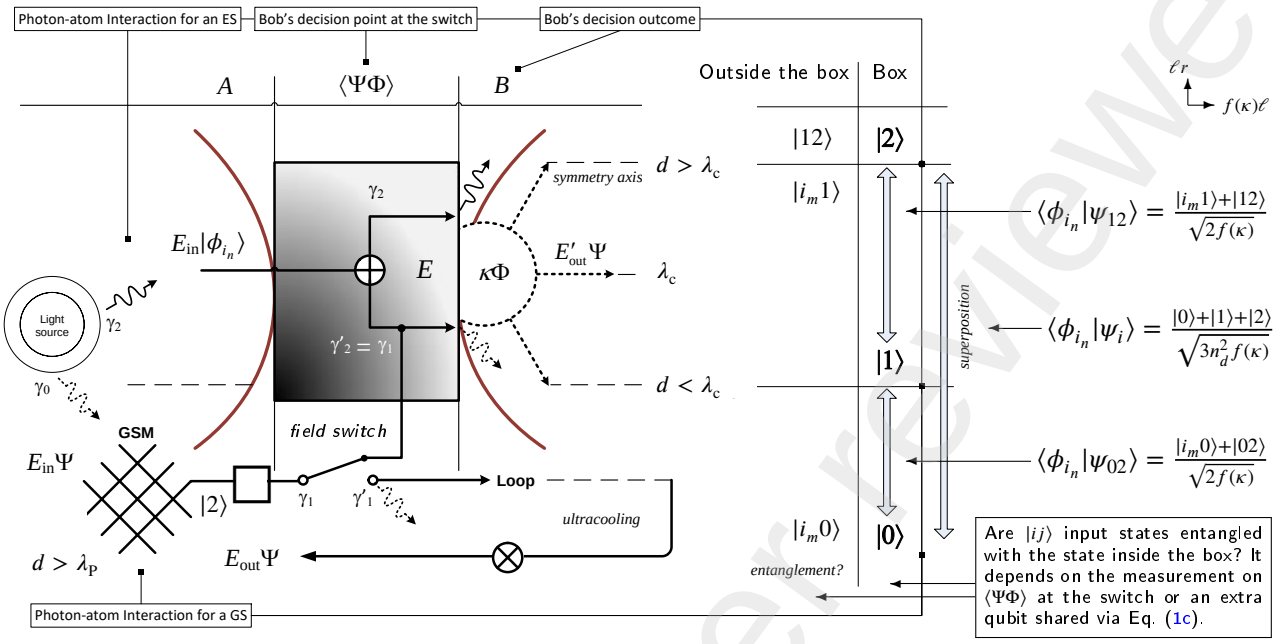

Fig. 4: QDF circuit. (Left) A laser cooling light is used to project photons onto particle space in a magnetic field (lattice) trap producing GSM, or a BEC [7, pp. 6–13]. (Left to middle) As in a scalar field transformation [52], by switching off the laser and magnetic fields, the GS is transformed into an ES, Sec. 2.2. An energy input-output (state) via the field switch corresponds to Eqs. (19)–(33). The complement of each state prior to a PT satisfying a TS, is denoted by its prime ($'$). The pre-switch side A has inputs from Alice, Eve and the audience as photons projecting onto Bob's field, affecting his state. The photonic projections on input states are γ_1 and γ_2, and the emissions are, respectively, γ'_1 and γ'_2, while γ_0 projections preserve a GSM. (Right to left) The state of a box is determined on the post-switch side B, where κ is applied. Scalar κ is obtained when Φ on side A is transformed to Ψ by the switch (GS $\leftrightarrow$ ES). A scalar matrix of input and output states (AB) is formed via κ. In this matrix, $|i\rangle$ in B relative to the two-qubit input $|ij\rangle$ from A to AB is measured (Table 1). From Eqs. (39)–(43), a positive correlation is on the $|\kappa^2_{\max}|$-scale denoting a box with the prize $|1\rangle$ entangled with state $|1_n\rangle$ of the nth participant who assumes the prize position $\mathfrak{r}$. An inverse correlation is between ES and GS, where a box content in either state correlates negatively with Bob's state, which is Alice's TS. (Right) Prize superposition is shown between boxes relative to particle interactions.

5.3. QDF circuit and the PDI choice

The entangled Bell states can be created for particle pairs in a quantum circuit [27–31]. This circuit is illustrated in Fig. 4, which corresponds to Figs. 1 and 2 events. The PDI choice (Sec. 3) of the circuit dynamics is illustrated in Fig. 3. The method to implement this circuit is presented in [7].

The circuit consists of a single-qubit gate (e.g., Hadamard gate), a two-qubit CNOT (controlled NOT) gate [31, 44], and a field switch to connect or disconnect the single-qubit gate. In Fig. 4, corresponding to Fig. 1 events, from left-to-right, the STs between E_{in} and E_{out}, Eq. (19), are measured by using photoprobes. On the left are laser projections which form an external field of photons and a GSM as the input to the circuit. This is comparable to the events of Fig. 1(b) to 1(a). The photoprobe's photon field projects its quantum state via $\mathbf{P}_{\Phi\Psi}$ from Eq. (21) between the gates. This is the PDI choice to measure a particle's state by a photoprobe. The probe's photon field falls into a superposition of the photons k momentum states generated by the gates. The single-qubit gate, denoted by a $\square$, transforms pairwise states via $f(\kappa)$. The circuit projects reversible transformations via $f(\kappa)$ on the pairwise states between particles. The single-qubit gate transforms $|ij\rangle$ into a superposition of states, which acts as a control qubit to a CNOT gate.

A solution to the quantum measurement problem of Eq. (27), is the PDI choice (Sec. 3) from $\mathbf{P}_{\Phi\Psi}$ in Eq. (21) on Θ, which satisfies the projection of a pairwise position in the direction of $\mathfrak{r}$. The initial projection is $\mathbf{P}_{\Phi\Psi}$, and the final projection is $\mathbf{P}_{\Psi\Phi}$ as our PDI choice illustrated between Alice, Bob and the prize in Fig. 3 (inspired by Refs. [12, 74]).

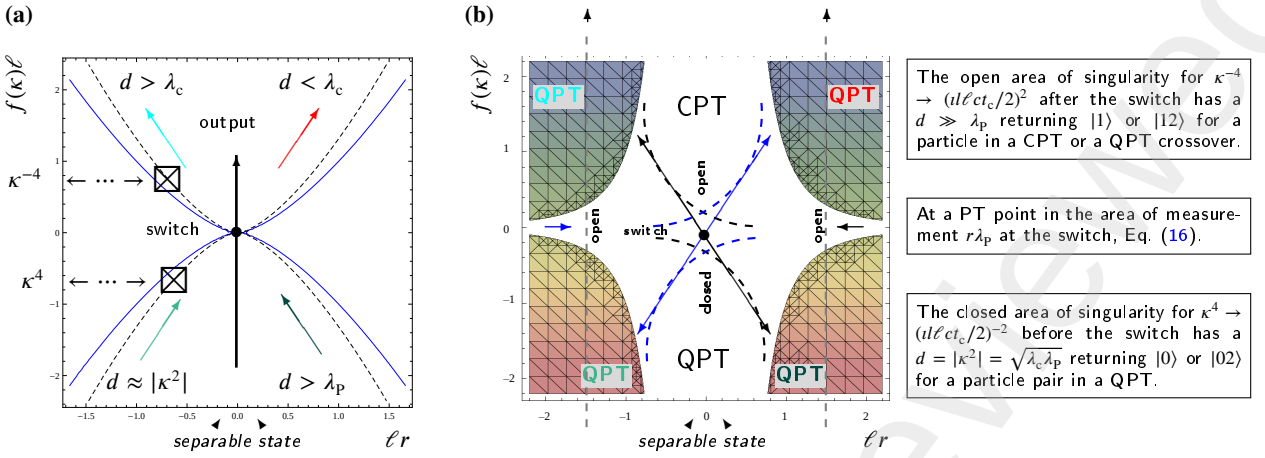

Fig. 5: A PT map for Fig. 3 participants to use κ within their interaction field $\Psi\Phi$ or $\Phi\Psi$. Plots **(a)** and **(b)** map to PTs in Fig. 4, on a scale of $|\kappa^2_{\min}|$ to $|\kappa^2_{\max}|$, relative to d, where $|\kappa^2_{\min}|$ returns a Planck length value between an input and an output state. Conversely, $|\kappa^2_{\max}|$ returns a great distance of $d \gg \lambda_P$ within the thermodynamic limit. Second order PTs, on a scale of $\kappa^{\pm 4}$, can occur and rise up to singularities within the GSM [22, 79]. This is shown in **(b)** as a closed/open area of singularity where a state is switched from the input to the output (a PT). The symmetry of diffusion, CPT (top mid-left), is a GSM (bottom-left), and the symmetry of QPT approaching a GSM (bottom right) is the CPT approaching 0 (top mid-right). The interactions area generating a GSM in **(a)** or **(b)**, is the closed area of singularity, $\kappa^4 \rightarrow (\imath\ell ct_c/2)^{-2}$, and t_c determines how long a particle pair can remain in a GS, or in state $|02\rangle$ which can be a crossover to a CPT from a QPT.

One would therefore, under a QDF transformation $\kappa\Phi \rightarrow \kappa^{-2}\Phi\ell r = |\Psi(\mathfrak{r}\mathbf{r})\langle\mathfrak{r}\mathbf{r}\rangle|$, expect

$$|\Theta(2\ell r)|_{\dot{l}} = \left|\left\langle 2\Delta d e^{-\imath\mathbf{k}_{i,j}\mathbf{r}}(2\mathbf{r}_{i,j})^{-1/2}\right\rangle\right| / |\langle\mathfrak{r}\mathbf{r}\rangle|^{1/2} = 2|\Delta d|/|\langle\mathfrak{r}\mathbf{r}\rangle|^{1/2} \in \left[1/2\sqrt{2}, 1\right], \tag{31}$$

where the scattering factor is $e^{-\imath\mathbf{k}_{i,j}\mathbf{r}} \approx 1$ via Alice's field. This observation is expected, provided that the wavelength of the radiation emitted from the ST is large for $\mathbf{k}_{i,j}|\mathbf{r}| = \lambda_c^{-1}|\kappa^2| \approx 0$ from Eq. (30), so that $d \approx |\kappa^2| = \sqrt{\lambda_c \lambda_P} \rightarrow 0$ and $\lambda_c \rightarrow 4d$ in Δd, before a PT. The emission is the result of the energy exchange between Alice (Eve) and Bob, Figs. 3(a, b). The field intensity radiation is emitted as a no prize state, or scattered as an energy decrease relative to $|\langle\mathfrak{r}\mathbf{r}\rangle|^{1/2}$.

Remark 10. The product states based on $|ij\rangle$ listed in Table 1, can be represented by qubits and reused to prepare the Bell states between game participants.

Remark 11. The QDF transform returns a probability amplitude of $|\psi_{ij}\rangle \rightarrow \Psi(\mathfrak{r}\mathbf{r}) \geq 2^{-1/2}$ for $\mathbf{r}$ or $\mathfrak{r}$ between two pairwise field points (superpositions), Eq. (14). From this, the minimum ST probability for a TS is $\min \mathcal{P}(\Psi \leftrightarrow \Phi) = 4|\Theta(2\ell r)|^2_{\dot{l}} \rightarrow 1/2$, according to Eqs. (17) and (31).

In Fig. 4, "control" is denoted by a dot • on the control qubit. The CNOT gate operates on a pair of particle states (a qubit pair). This gate can be used to entangle and disentangle Bell states. These operations can be expressed as a direct sum $\oplus$, or a tensor product $\otimes$ of two inputs between states $|\psi\rangle$ and $|\phi\rangle$, followed by the field switch. The direct sum returns a target qubit as an assumed prize state $|i_n\rangle$ by Bob, Table 1. A PT occurs per field switch as a tensor product $|\psi\rangle \otimes |\phi\rangle$, or $|\psi\rangle \oplus |\phi\rangle$, given $\mathbf{r}_{i,j}$ and $\mathbf{k}_{i,j}$ values. The control qubit in CNOT remains unchanged and is in sate $|0_m\rangle$ for a box known or unknown to Bob (steps 4-7). The target qubit flips, only if the control qubit is $|1_m\rangle$ set by Alice for a QPT or its crossover to a CPT, as her TS [85]. This reversible qubit mapping can be retrieved to determine i.

In the method [7], examples of Bell states have been implemented by the QDF circuit, corresponding to Table 1 prediction outcomes, and Fig. 4 question on entanglement. The circuit measurement results for distinguishing entangled states are listed in [7, Tables 4 and 5]. For example, a third party Eve who holds nothing of value can have any of her nonorthogonal states paired and entangled with other parties, according to Eq. (1c), as a combination of orthogonal and nonorthogonal states. This is by sharing an extra qubit in any nonorthogonal state of $|2\rangle$, as one of her states [18].

Hence, her qubit complements nonorthogonality of two or more states to an orthogonal state, which yields information about $\mathfrak{r}$ with certainty. Eve here, is the vital party who can communicate the result to any party, see Fig. 3.

For all particle pairs in the QDF circuit, the qubits via $\langle f(\kappa)\mathcal{T}(\mathbf{k})|\mathbf{r}\rangle$ in Eq. (13), transform into a sum of superpositions. From Eqs. (2)–(9), (12)–(27), this is the sum of tensor products ± operations for maximally entangled states. If the assumption of including a third party or an extra qubit from Eq. (1c) is to be ignored, then via $\mathbf{P}_{\Phi\Psi}$,

$$\sum_{1\leq \dot{l}\leq \mu_{ij}}^{3\leq \mu_{ij}<\infty} \left| \overbrace{\frac{\langle 2\mathbf{r}_{i,j}|f(\kappa)\ell\psi_{ij}\rangle}{|\langle \mathfrak{r}\mathbf{r}\rangle|^{1/2}}}^{\Theta(2\ell r)} \left(|0_m i_n\rangle \pm |1_m i'_n\rangle\right) \right|_{\dot{l}}, \tag{32}$$

where i'_n is the negation of i_n as the target qubit. For any $\dot{l}$ field position(s), there is a temporal QDF correlation function $|\Theta(2\ell r)|_{\dot{l}}$, which evaluates $\mathbf{r}_{i,j}$ as $\mathbf{k}_{i,j}|\mathbf{r}| \to |\mathbf{k}\mathbf{r}| \to 1$ via κ from Eq. (6). Any value of $\lambda_c > 1$ that satisfies $d \to 1$, denotes an energy increase revealing $\mathfrak{r}$ in $|\langle \mathfrak{r}\mathbf{r}\rangle|^{1/2}$ from the sum of $|\Theta(2\ell r)|_{\dot{l}}$, which is expressed in Eq. (33).

In Eq. (32), the circuit outputs a Bell state per $\dot{l}$-field position, given a pair of qubits (inputs). The μ_{ij}-minimum in the sum denotes the interactions of a particle pair map to the minimum possible number of entangled states by a third particle, e.g., Eve sharing information with Bob. The bases of the tensor products match with $|i_m i_n\rangle$ projections in Table 1, except for $|02\rangle$ and $|12\rangle$. To include the target qubits from $|02\rangle$ and $|12\rangle$, Eq. (32) is complemented by Eq. (39), which denotes any of the output states shown on Fig. 4 right side.

Example 6. In Fig. 3(c), for $|\Theta(2\ell r)|_{\dot{l}} \to 1/2\sqrt{2}$, d tends to 0 in Δd from Eq. (31), which denotes *separable states* [31], as $|\langle \mathfrak{r}\mathbf{r}\rangle|^{1/2} \in [1, \sqrt{2}]$ is detected between Bob and the prize. Meanwhile, λ_c tends to 1 as a finite value bordering a PT singularity at a critical point (pre-switch). The singularity forms as λ_c diverges to ∞ in Δd. This is expressed in Eq. (30) and illustrated in Fig. 5. The value $1/2$ as a factor of $1/2\sqrt{2}$ is the expected superposition, as $|\langle \mathfrak{r}\mathbf{r}\rangle|^{1/2} \to 1$ in Eq. (32). The value $2^{-1/2}$ as the remaining factor of $1/2\sqrt{2}$ is the quantum mechanical expectation value of the tensor product $|i_m i_n\rangle$ in the Bell singlet state. The fraction $1/2\sqrt{2}$ can be factored in, to encode a qubit into entangled states of triplet qubits. This can be used to correct a possible qubit error in the circuit [44], as Bob decides or switch for his TS.

Example 7. A strong prediction in a QDF circuit is a value of $|\langle \mathfrak{r}\mathbf{r}\rangle|^{1/2} \to 1$ for $|\Theta(2\ell r)|_{\dot{l}} \to 3/2\sqrt{2} \approx 1$. This covers three out of four Bell states simultaneously. As $d \to 1$, $|\langle \mathfrak{r}\mathbf{r}\rangle|^{1/2}$ tends to $\sqrt{2}$, and from Eqs. (26)–(30), $2|\langle f(\kappa)\ell\rangle|\lambda_P = 2\kappa^2\lambda_P \in [2\lambda_P, 1]$, as $\lambda_c \in [2d, \infty]$. Here, an energy increase is expected as Bob's assumed prize position $\mathfrak{r}$, i.e., $\langle \mathfrak{r}\rangle$ from $\langle \mathbf{r}_{i,j}\rangle$ correlates with $\langle \mathbf{k}_{i,j}\rangle$ from Eq. (4).

The correlations sum between pairwise states via projection $\mathbf{P}_{\Phi\Psi}$ is

$$\left|\sum_{\dot{l}=1}^{\mu_{ij}} \langle \mathbf{k}\mathbf{r}\rangle_{c_{\dot{l}}}\right| = \left|\sum_{\dot{l}=1}^{\mu_{ij}} [2\Theta(2\ell r)]_{\dot{l}}\right| \gtrsim 2, \tag{33}$$

which is derived from Eqs. (18) and (32). For a particle pair interacting at $\dot{l}$, given $|\langle \Phi|\mathbf{k}\mathbf{r}|\Psi\rangle| \to 0$, leads Eq. (5) to break the ultimate minimum uncertainty such as establishing zero uncertainty with maximum entanglement [89], Remark 7. Here, the focus shifts from the probabilistic picture 2.2.1 measuring HUP products, to the deterministic picture distinguishing Bell states, Sec. 2.2.2, Remark 5. In addition, ST probability values $< 1/2$ are returned which validate Eq. (17) expected values in preparing superposition and Bell states. In case of $\min f(N) < 3$ for a single interacting pair, $\min \mu_{ij} = 1$, assuming $|\langle \Phi|\mathbf{k}\mathbf{r}|\Psi\rangle| \geq 1/2$ satisfies superposition, Bell's inequality is not violated. This satisfies Bob's TS as a prize win, if Bob and the prize interact directly, or via Eve as uncorrelated and unentangled (separable) states. However, in case of $\min f(N) = 3$, Bell's inequality is violated, according to Θ.

Remark 12. The Θ measure, based on $2\ell r \leq l\ell ct_c$, gives rise to the number of κ operations needed between two field points, $4|\langle \Theta(2\ell r)\Theta(l\ell ct_c)\rangle| \leq 1/2$. This determines separable states against Bell states.

As shown in Fig. 3(d), the propagation factor $e^{\imath\mathbf{kr}}$ occurs after scattering, $e^{\imath\mathbf{k}_{i,j}\mathbf{r}}$ in Eq. (31), where separable states from the photoprobe momenta is measured, Eq. (22). Zero superposition is also shown in Fig. 3(d), which denotes every plane in a photoprobe plane-wave orthogonal to the direction of its propagation (along $\mathbf{k}$), Eq. (23). The value of Θ depends on the least uncertainty, as $2|\langle\mathfrak{r}\mathbf{r}\rangle|^{1/2}\kappa^{-2}$ tends to $|\langle\Phi|\mathbf{kr}|\Psi\rangle| = 1$ from Eqs. (5) and (27). The Θ value changes if entanglement and PT decay across time t_c as a temporal measure between two field points $2\ell r \leq l\ell ct_c$, Eqs. (14)–(20). Hence, the photoprobe interacting with a particle pair might not entangle and merely be in superposition.

Figure 3(e) shows the cross-section of state projections and prediction for all pairwise interactions from Figs. 3(a)–(d). Each expected pairwise interaction for a PT is measured relative to the magnitude of its temporal correlation from Eq. (31), i.e. $\langle 4\Delta d e^{-\imath 2\mathbf{k}_{i,j}\mathbf{r}}\rangle|\Theta(2\ell r)\mathbf{r}|^{-1} \in [-2\sqrt{2}, 2\sqrt{2}]$. This is expressed as the intersecting areas of information between axes $\ell\lambda_c$ and $\Theta(2\ell r)$ in Fig. 3(e).

The magnitude of expected positions of the prize correlated to Bob's position, as a point of entanglement, under the κ-based field transformation from Eq. (31), can be written as

$$\lim_{|\mathbf{kr}|\to 1}\left|\frac{\kappa^2\sqrt{|\langle\mathfrak{r}\mathbf{r}\rangle|}e^{\imath\mathbf{k}\mathfrak{r}}}{\langle\mathbf{r}\Delta d e^{2\imath\mathbf{k}_{i,j}\mathbf{r}}\rangle}\right| = \frac{2\sqrt{|\langle\mathbf{k}\mathfrak{r}\mathbf{k}\mathbf{r}\rangle|}}{e^{-\imath\mathbf{k}(\mathfrak{r}-2\mathbf{r})}} \leq \frac{1}{|\Theta(2\ell r)|_l^{\prime}}, \quad \min f(N) = 4 \text{ for } \mu_{ij}. \tag{34}$$

The result can be evaluated relative to R and Θ, where $\mathbf{P}_{\Phi\Psi}$ and a PT (an energy shift) occur. The more quantum information shared with Bob, the greater the radius of the field containing information about $\mathfrak{r}$.

6. System thermodynamics

The system thermodynamics describes the events of the QDF circuit, as discussed in Sec. 5, Eqs. (23)–(34).

6.1. Phase transition via QDF products

A PT occurs from the external photon field as $|\psi\rangle \otimes |\phi\rangle$ or $|\psi\rangle \oplus |\phi\rangle$, given $\mathbf{r}_{i,j}$ and $\mathbf{k}_{i,j}$ in Eq. (22). The direct sum and the tensor product of the atomic and quantum spaces, are respectively $\mathcal{S}_{\mathbf{r}}$ and $\mathcal{S}_{\mathbf{k}} \subset \mathcal{S}$, applied to one quantum particle interacting with an atom, and to two or more interacting quantum particles [94]. The tensor product captures the interaction on condensate cases where a GSM is observed due to a pairwise particle interaction. As Bob interacts with a quantum particle accessing the shared quantum information from that particle, he pairs his state with the no prize state. Bob can then predict which box has the prize, as his TS to attain, from a diffused product which also has the opposite TS measurable from the QDF intensity products as follows.

The field intensity I is measured relative to the QDF metric space, its scattering factor $e^{2\imath\mathbf{k}_{i,j}\mathbf{r}}$, correlation function, and λ_c from Eqs. (6)–(18) and Eqs. (24)–(34). The intensity characterizes a PT on even orders of magnitude $|\kappa^4|^2$, where the prize state is determined relative to Bob's position $\mathbf{r}$. From Eq. (28), Ψ via $f(\kappa)$, and λ_c satisfies

$$I \propto f(\kappa)|\langle\Psi\rangle|^2/\lambda_c^2 = \left(|\kappa^4|e^{\imath\mathbf{k}\mathfrak{r}}\right)^2/4\pi|\mathbf{r}|^2, \tag{35}$$

due to a photon-atom interaction. This forms a direct sum $|\psi\rangle \oplus |\phi\rangle$ of the two fields Ψ and Φ, relative to E_{in} and $\langle E_{\text{out}}\rangle$. The direct sum stacks up the value of each observable (a state), so that the quantum states can be separable on the output side as particles diffuse and expand from their product [94]. This measures a particle state relative to λ_c.

Position $\mathfrak{r}$ relative to t_c, depends on the sum of revolutions of a unit circle (frequency) based on the observable of each interacting particle pair. The sum for the prize is $4\pi r^2 = 4\pi$ as $r = 1$, Eq. (35). For a pairwise particle interacting with the prize, the sum is $16\pi^2$. This is the quantum information shared about $\mathfrak{r}$ via $\mathbf{k}$. Given the quantum separation from the photoprobe momenta, Eqs. (22) and (29), and the photon propagation in Eq. (6), the inverse QDF intensity is

$$I' \propto f(\kappa)|\langle\Phi\rangle|^2\lambda_c\lambda_P = 16\pi^2/\left(|\kappa^4|\mathbf{k}_{i,j}e^{\imath\mathbf{k}_{i,j}\mathbf{r}}\right)^2, \tag{36}$$

where the information on $\mathfrak{r}$ is shared within the pairwise interaction area $|\langle\mathfrak{r}\mathbf{r}\rangle|$ under a curve between two boxes, see Example 2. The prize state propagates in this area, as it travels at a distance of $\sqrt{|\langle\mathfrak{r}\mathbf{r}\rangle|} \to \mathbf{r}_{i,j} \leq d \to |\mathfrak{r}|$ via $|\Delta d|$, Eqs. (5) and (24). This propagation comes from the quantum Fourier transform on qubits [31, 52], where ≥ 3 qubits are used, Sec. 5.3. Multiple qubit rotations about 2π angles are expected denoting particle energy exchange throughout the photon propagation for the prize. This propagation satisfies the TSs for Bob and Alice for "an attainable one prize

state" from Sec. 1, by which, Alice or Bob wins on the QDF scale based on the product of *prize-state phase shifts* in determining $\mathfrak{r}$. This is achieved by the *photon propagator* for the prize, which is scaled to

$$\Gamma = \overbrace{\frac{2\min\mu_{ij}}{\min\mathcal{P}(\Psi\leftrightarrow\Phi)}}^{3\times4=12}\int_{\mathcal{S}}|\Phi\Psi(\mathfrak{r})|^2\,\mathrm{d}\theta_k^2\,\mathrm{d}\theta_r\,\mathrm{d}\theta_{\mathfrak{r}} = 3\sqrt{\pi},\ \text{ where }\int_{\mathcal{S}}\equiv\int_{\mathcal{S}_{\mathbf{k}}}\int_{\mathcal{S}_{\mathbf{r}}}\int_{\mathcal{S}_{\mathfrak{r}}}\text{ as }\int_{4\pi}^{0}\int_{16\pi^2}^{4\pi}\int_{0}^{16\pi^2}, \tag{37}$$

and $|\Phi\Psi(\mathfrak{r})|^2$ with an ST probability $\mathcal{P}(\Phi\Psi(\mathfrak{r})) = 1/2$ associated with the product of a rotational phase shift $e^{-\theta_k}e^{-|\theta_{\mathfrak{r}}-2\theta_{\mathbf{r}}|}$, which denotes pairwise photons propagate with a magnitude of $|\mathfrak{r}-2\mathbf{r}|$ and $|\mathbf{k}|$ through game space $\mathcal{S}$. This depends on the $\mathbf{k}$-direction, as defined by the angle θ. A strong prediction of $\mathfrak{r}$ can be made by computing the square root of the field components in Eqs. (34)–(37). This returns a dimensionless field intensity product

$$\lim_{|\mathbf{kr}|\to1}\Pi_{|1\rangle} = \frac{\sqrt{II'|\langle\mathfrak{rr}\rangle|}}{\Gamma d} = \frac{2}{3}\frac{\sqrt{|\langle\mathfrak{rr}\rangle|}}{d\,e^{\imath\mathbf{k}(\mathfrak{r}-\mathbf{r})}} \in \left[\frac{2}{3},1\right],\ \text{where }\langle\mathfrak{r}|\mathcal{T}(\mathbf{r})|\mathbf{k}\rangle = e^{\imath\mathbf{k}(\mathfrak{r}-\mathbf{r})}/|\mathfrak{rr}|^{3/2}, \tag{38}$$

and for the scattering phase shift, $\mathbf{k}(\mathfrak{r}-\mathbf{r})$, $e^{-\imath\mathbf{k}(\mathfrak{r}-\mathbf{r})}\approx1$, as $d\to|\mathfrak{r}|$ tends to 1 from $|\langle\mathbf{r}\mathfrak{r}\rangle|^{1/2}$ in Eqs. (24)–(34). The ST operator $\mathcal{T}(\mathbf{r})$, shifts particles and fields to a zero superposition with a probability of $\geq 2/3$ in finding $\mathfrak{r}$. This is if energy shifts, based on ΔE in Eq. (9), are observed between the energy input of e.g., Eve from Eq. (1b), complementing other states of particles as the expected energy output $\langle E_{\text{out}}\rangle$ in the QDF circuit. Other values of $\mathfrak{r}$ satisfy superposition or entangled Bell states from the circuit.

An intensity product $\Pi_{|0\rangle}$, by measuring $\Pi_{|1\rangle}$, maps to a closed area of singularity for κ^4, as $d = |\kappa^2| = \sqrt{\lambda_{\text{c}}\lambda_{\text{P}}} \in (\lambda_{\text{P}},1]$ at the pre-switch, which returns $|0\rangle$ or $|02\rangle$ for a particle in a QPT, Fig. 5(b). Another field intensity product is $\Pi_{|2\rangle}$, which denotes a continuous probability density on a prize state, as $d>\lambda_{\text{c}}>1$, which maps to an open area of singularity. The product $\Pi_{|2\rangle}$ contributes to a continuous QPT, as $d>\lambda_{\text{P}}$ (like in $\Pi_{|0\rangle}$), otherwise a crossover to a CPT, Eq. (1). Thus, $\Pi_{|0\rangle} = 1-\Pi_{|1\rangle}$ denotes the complement of product $\Pi_{|1\rangle}$, and $\Pi_{|2\rangle} = 1-\{\Pi_{|0\rangle},\Pi_{|1\rangle}\}$ denotes the complement of a no prize state or otherwise.

From Eqs. (1), (10)–(31), the superposition from Bob and others as a photon, a photoprobe, and an atom, is projected onto the prize state between the boxes, Fig. 4,

$$f(\kappa)\Phi \xleftrightarrow[\psi_i(\mathfrak{r})]{\mathbf{P}_{\ell'}} f(\kappa)\Psi = \begin{cases} \langle\phi_{i_n}|\psi_{ij}\overset{\mathbf{P}_{\Psi(\mathfrak{rr})}}{\longrightarrow}\psi_{i_m2}\rangle = \left[|i_m i_n\rangle + |i_m 2\rangle\right][2f(\kappa)]^{-1/2}, & \text{(39a)}\\ \langle\phi_{i_n}|\psi_{ij}\overset{\mathbf{P}_{\Psi(\mathfrak{r})}}{\longrightarrow}\psi_i\rangle = \left[|0\rangle+|1\rangle+|2\rangle\right][3n_d^2 f(\kappa)]^{-1/2}, & \text{(39b)}\end{cases}$$

where Bob can predict $\mathfrak{r}$ via $f(\kappa)$ based on: Eq. (39a) as projection $\mathbf{P}_{\Psi(\mathfrak{r})}$ denoting superposition, or, Eq. (39b) as $\mathbf{P}_{\Psi(\mathfrak{rr})}$ denoting Bob's entanglement with the prize, Eq. (27). This TS is predicted if the correlation between Bob, Alice and the prize observables are measured from Eq. (19) as

$$|E\langle f(\kappa)\ell'\rangle| = |E_{\text{in}}\langle\mathbf{kr}\rangle_{\text{c}}|\xrightarrow{\cdot\mathbf{r}_{i,j}^2}|E_{i_n}\langle\mathfrak{rr}\rangle|\xrightarrow{\cdot\mathbf{k}_{i,j}^2}|E_{\text{out}}\langle\mathbf{k}\mathfrak{r}\rangle|, \tag{40}$$

where $|E_{\text{out}}\langle\mathbf{k}\mathfrak{r}\rangle|\to E\Pi_{|1\rangle}$. The output state can be determined from the correlation and particle interaction relative to 6 particle positions, Examples 3–5. This gives a positions ratio of $\alpha^2 = \{4\mathbf{k}_{i,j}:2\mathbf{r}_{i,j}\}$, relative to the probability density function $\varrho = \varrho(\mathbf{k}_{i,j})$ or $\varrho(\mathbf{r}_{i,j})$. The output is a low or high density of states projected by an interacting particle pair onto the prize state entangled in the lower and upper bounds of κ, $|\kappa^2_{\min}|$ and $|\kappa^2_{\max}|$, respectively.

Each QDF function is evaluated on either side of a double-sided arrow defining the κ-limit, as shown here:

$$f(\kappa)\overbrace{\lim_{|\mathbf{kr}|\to1}\langle\varrho(\mathbf{k}\mathfrak{r})\rangle}^{|\langle\Psi|\Phi\rangle|^{\pm2}=\varrho} = \begin{cases} \left|\kappa^2_{\min}\right|\varrho(\mathbf{k}_{i,j}) = \left[2\int_{\mathcal{S}_{\mathbf{k}}}\mathrm{d}k\left|\kappa\Phi\Psi(\mathfrak{r})\phi_{i_n}\right|/\mu_{ij}\right]^{1/2}\xleftrightarrow{|\kappa^2\alpha|^{-2}}\min\mu_{ij}\mathbf{r}_{i,j}[2\langle\lambda_{\text{c}}\rangle]^{-1}\gtrsim0,\\ \left|\kappa^2_{\max}\right|\varrho(\mathbf{r}_{i,j}) = \left[\min\mu_{ij}\int_{\mathcal{S}_{\mathfrak{r}}}\mathrm{d}\mathfrak{r}\left|\kappa\Psi(\mathfrak{rr})\psi_{ij}\right|\right]^{1/2}\xleftrightarrow{|\kappa^2\alpha|^2}2\langle\lambda_{\text{c}}\rangle[\mu_{ij}\mathbf{r}_{i,j}]^{-1}\leq2,\end{cases} \tag{41}$$

where $\langle\lambda_c\rangle \approx 3d$ is by averaging the non-divergent values of λ_c on the interval $[2d, 4d]$ from Eq. (30). The arrow's left side satisfies QDF functions $f(\kappa)\Psi$ and $f(\kappa)\Phi$ from Eq. (39), which determines a PT by taking the double-square root of the state quantities under the transformation $|\mathbf{kr}| \to 1$. The discrete energy values of a GS or ES hold true on the arrow's right side based on $|\kappa^2\alpha|^{\pm 2}$ as the states are uniformly distributed within the κ-limit. The upper and lower bounds of κ are evaluated by plugging in values from Eqs. (22)–(30). As the information on $\mathfrak{r}$ is shared with Bob via pairwise interaction, Eqs. (31)–(38), $|\kappa^2_{\min}|\varrho(\mathbf{k}_{i,j})$ can be evaluated by applying the least uncertainty $\mathbf{r}_{i,j} = 1/2\mathbf{k}_{i,j}$ to a min $f(N) < 4$ in min μ_{ij}, Sec. 5.3. This returns $|\kappa^2\alpha|^{-2} \in (0, 1]$, where the upper limit denotes $d = 1/2$, as a superposition between a particle pair. For a min $f(N) = 4$, and $\mathbf{r}_{i,j} \geq 1/2\mathbf{k}_{i,j}$, $|\kappa^2\alpha|^2 \leq 2$ is returned. Any evaluation of κ and its limit, based on $\lambda_c \in (d, \infty]$ for $f(N) > 3$, falls within the bounds of $|\kappa^2_{\min}|\varrho(\mathbf{k}_{i,j})$ and $|\kappa^2_{\max}|\varrho(\mathbf{r}_{i,j})$. Moreover, the expected probability of an output state can be measured by observing the expected area of interaction relative to the open and closed singularities within the κ-limit, as shown in Figs. 4 and 5.

6.2. Overview of the κ-limit

As shown in Fig. 5, a field switch satisfying a PT, forms a hyperbola of particle momenta in units of λ_P^{-1}, Eq. (13), with a ratio of $|\kappa^2_{\max}| : |\kappa^2_{\min}|$, where $|\kappa^2_{\max}|$ values form a divergent concave curve. For instance, $|\kappa^2_{\max}|$ returns values of $d = \lambda_c|\langle\mathfrak{r}\mathbf{r}\rangle/\kappa^4| \gg \lambda_P$, denoting $|1\rangle$ or a product state $|12\rangle$ for a particle in a CPT, or a QPT crossover. Conversely, $|\kappa^2_{\min}|$ forms a convergent convex curve approaching $d = \lambda_c^{-1}|\kappa^4| = \sqrt{\lambda_c\lambda_P} \approx \lambda_P$, or singularity, as a continuous PT [77–80]. This returns $|0\rangle$ or a product state $|02\rangle$ for a particle pair in a QPT. The open singularity at $d > 1$ maps to a possible energy release from a near-singularity geometry and a dense mass of BEC formed at levels of GSM. This formation can be observed at Bob's decision point (at the switch), which is the amount of information taken from the sum of energy input of N participants, thereby levels of equivalent energy release on the output side, Eq. (40).

On the one hand, the information gathered at distance $d > 1$, equivalently originates from the uncertainty measure of the observable $\mathcal{O}$ in Eq. (22) for each interacting pairwise particle falling into a GS. A particle can be continuously trapped in one box (Fig. 4) while entangled with Bob as a pair denoting the no prize state, see Example 3.

On the other hand, the information gathered at zero distance $d = 0$, denotes a separable state of the QDF on the input side or matrix A coupled with the prize's state on the output side or matrix B after the switch, Figs. 4 and 5. This coupling is based on Fermi's golden rule [80]. However, the quantum information is obtained on the closed singularity at $d \in (\lambda_P, 1]$, which returns $|0\rangle$ or $|02\rangle$ for a particle in a QPT. For both cases, the rule implies that the ST probability per unit of time from the input state $|i_m\rangle$ to a set of final states $|i_n \to i\rangle$ of a box or Bob (who could be entangled with the prize state), as a constant. This rule can be written as

$$\mathcal{P}(\Phi \to \Psi) = \min f(N)AB\left(f(N)\left|\Delta\kappa^2\ell\right|\right)^{-1}, \text{ and } \quad \left|\Delta\kappa^2\right| = \left|\kappa^2_{\max} - \kappa^2_{\min}\right|, \tag{42}$$

where $|\Delta\kappa^2\ell|$ is the matrix element in a QDF density matrix $\rho_{AB} = AB|\Delta\kappa^2\ell|^{-1}$, as discussed in Sec. 7. The final and initial states are coupled on a magnitude of $[1, \sqrt{2}]$-positions relative to μ_{ij}, Eqs. (25)–(27). This equation projects the ST probability approximation for a PT. This is the projected output state after quantum decoherence which occurs at the final model step. This rule is further applied in Sec. 7, to determine the ST probability values from Eq. (17).

The obtainable information at distance $d \in (0, \sqrt{\lambda_c\lambda_P} \to 1]$ is from the open and closed areas of singularity, where a particle contributes its energy to a QPT $\leftrightarrow$ CPT. These areas have been delimited by a rising or falling curve denoted by $\boxtimes$ in Fig. 5(a). The curves correspond to Fig. 5(b) areas between the input and the output that can be coupled with one another as $|ij\rangle \leftrightarrow |i\rangle$. The input-output data are plotted on axes ℓr and $f(\kappa)\ell$. The limit scales up to any closed or open areas of singularity in the map $\kappa^{\pm 4} \to (\imath l\ell c t_c/2)^{\mp 2}$, where $\ell r \leq 2\ell c t_c$, Eq. (20). This limit determines via t_c, how long a particle pair can remain in a GS, ES, or entangle between the GS and ES before a κ operation, as a PT.

Bob at the switch measures $\mathfrak{r}$ at intervals of $\kappa^{\pm 4dk}\alpha^{\pm 2} = \left(\sqrt{2|\mathfrak{r}|}\kappa\alpha\right)^{\pm 2}$, Eqs. (25)–(27) and (41). From the ratio $|\kappa^2_{\max}| : |\kappa^2_{\min}|$, the entangled state between Bob and the prize can be determined within the scalar limit

$$\lim_{d\in(0,1]}\left|\Delta\kappa^2\ell\right| = \sqrt[4]{\left|\kappa^2\left(\min\mu^2_{ij}|\psi_{ij}|^2 - 2|\phi^2_{i_n}\mathfrak{r}|^2\mu^2_{ij}\right)\right|} = \left|\kappa^4\alpha^2 - \kappa^{-4}\alpha^{-2}\right| \lesssim 2, \tag{43}$$

where $|\Delta\kappa^2|$ is for an ℓ-transformation $|\kappa^2\Psi(\mathfrak{r}\mathbf{r})| \to 2|\Phi\Psi(\mathfrak{r})| = 1$ with a $\mathcal{P}(\Phi\Psi(\mathfrak{r})) = 1/2$, across t_c at the switch.

Example 8. A spontaneous symmetry breaking [82] is formed as d tends to 1, Fig. 5, where a QPT to a CPT occurs as $\lambda_c \in [\lambda_p, 2d]$ from Eqs. (18) and (31). A result of $|\Delta\kappa^2\ell| \approx 2$ satisfies the GS and ES discrete energies, as well as the double square root of the state quantities. The result denotes ϕ_{i_n} is projected by Alice onto $S_{\mathfrak{r}}$ of the prize in superposition. If Bob assumes the prize state by entangling his state $|i_n\rangle$ with it, then $|\phi_{i_n}\rangle = |\psi_{ij\to 12}\rangle$ projects $i = 1$, Eq. (39). A result of $|\Delta\kappa^2\ell| < 2$, denotes the information on $\mathfrak{r}$ is shared with Bob at $d \leq 1$. This is satisfied by $\lambda_c \in [2d, 4d]$ from the input-output state coupling, Eq. (42), within the open-closed areas of singularity.

6.3. Measurement overview

From Secs. 3–6 discussions, the input-output state coupling of a particle via projection (PDI), relative to particle pairing from Sec. 4.2, gives the least uncertainty in the measurement of S. This was evaluated by measuring incompatible observables $\mathbf{k}$, $\mathbf{r}$ and $\mathfrak{r}$ from a single-field metric space, to a compatible measurement of $\mathfrak{r}$ based on its correlation with $\mathbf{k}$ and $\mathbf{r}$ via κ from the QDF metric (fmv) space. Here, for a given number of pairwise inputs under the transformation $|\mathbf{kr}| \to 1$ via $f(\kappa)$, the input-output state coupling is reversible and consistent with the history of STs contributing to a PT within the thermodynamic limit. This was shown in Secs. 4.2–5.3, where measuring an expected outcome of $f(\kappa)\langle\mathbf{kr}\rangle$ is reciprocal, and reversible by accessing and retrieving the quantum information from $f(N)$-qubit gates in a QDF circuit. This measurement method, as implemented in [7], is applied to this circuit with proof as follows.

7. QDF theorem, proof and application

There are N participants with access to quantum information about $\mathbf{k}\mathfrak{r}$ from Eq. (40). By using this information, one can predict the state of each box content given three possible input states $Z \in [1, 3]$. A pair of input states from a pair of particles, can pair up with another particle state. An output state via $f(\kappa)$ acting on $\mathbb{F}$ can then be predicted.

Theorem. *A κ-based field transforms $\kappa\Phi$ to $|\Psi(\mathfrak{r}\mathbf{r})\langle\mathfrak{r}\mathbf{r}\rangle|$. The ST probability of state i from $2|\mathbf{r}| \overset{\mu_{ij}}{\longleftrightarrow} \{|\mathfrak{r}|, 2|\mathfrak{r}|\}$ positions for three possible input states is $\mathcal{P}(\Phi \to \Psi) > 1/2$. This is a classical state predicted from quantum state $|i_n\rangle$ as $\delta \to 1$ is observed on a magnitude of $|\kappa^2|\varrho \leq 2$.*

Proof. The product of matrices A and B is a double-field matrix AB. A field switch in Figs. 1–5 denoting a PT, causes a field transformation within the κ-limit, Eq. (43). This transformation can be expressed in a density matrix

$$\rho_{AB} = AB\left|\Delta\kappa^2\ell\right|^{-1} \longrightarrow B\left|\Delta\kappa^2\ell\right|^{-1}, \tag{44}$$

where $A = \begin{bmatrix} 1 & 0 & 1 \\ 1 & 1 & 1 \\ 1 & -1 & -1 \end{bmatrix}$ and $B = \begin{bmatrix} 1 & 0 & 1 \\ 1 & 0 & 1 \\ 1 & 0 & -1 \end{bmatrix}$, given d in the complex plane is projected from the area of particle interactions, n_d^2, obtainable from Eq. (10). In Fig. 5, $\iota^2 = -1$ in A or B denotes the switching event from $A \to B$ via κ for a GS. However, $\iota^4 = 1$ is for an ES. The double-field matrix for the GS and ES is

$$AB = \begin{bmatrix} 2 & 0 & 0 \\ 3 & 0 & 1 \\ -1 & 0 & 1 \end{bmatrix}. \tag{45}$$

The left and right column elements in A and B are the basis states between the input and output of the QDF circuit. Quantum gates transform states via the QDF switch elements in the middle. In a QDF density matrix, Eq. (54), the normalization factor $1/\sqrt{2}$ from a gate transformation is omitted. This determines a separable state of product $|ij\rangle$ relative to a Bell state on the output side via $\mathcal{O}$, Eqs. (22)–(34). Instead, an ST probability of $\mathcal{P}(\Phi \to \Psi) \geq |\Theta(2\ell r)|_l^2$ from Eq. (32) is valid under the transform $\kappa\Phi \to 2\kappa^{-2}\Phi\ell r = |\Psi(\mathfrak{r}\mathbf{r})\langle\mathfrak{r}\mathbf{r}\rangle|$. For determining an ST for a TS, the κ-operation on the AB matrix elements is observed based on the inverse of the κ-limit from Eqs. (42) and (43), as

$$\left|\Delta\kappa^2\ell\right|^{-1} = f(N)\mathcal{P}(\Phi \to \Psi)/Z, \tag{46}$$

where Z is the number of possible energy inputs (states) from $Z \in [\min f(N), f(N)]$ participants in the matrix left column. The inputs can be switched to one or two outputs (box(es)) in the matrix right column. This column denotes one of the outputs to be with a prize (steps 5–7). The prize position $\mathfrak{r}$ can be predicted by measuring the ST probability of each state via κ in the matrix. The matrix can contain a negative number $\iota^2 = -1$ denoting an ST at a QPT for an expected TS, Eq. (17). This ST occurs within a GS between Bob's state $|0_n\rangle$ correlating with the no prize state $|0\rangle$ of a box. Bob can then predict the final state $|1\rangle$ of the remaining box (output) with the prize, as his TS, Eq. (21).

For a prediction, the ST probability $\mathcal{P}(\Phi \to \Psi)$ via κ must be computed. This prediction needs two computational steps: 1- measure the fmv, 2- measure the decomposition of fmv components into a single equation for $\mathcal{P}(\Phi \to \Psi)$.

Two photons from fields $\gamma_0\Psi$ and $\gamma_1|\phi_{i_n}\rangle$ are projected onto an atom's field as the matrix input, Fig. 4. The photons within their probe's field read the atom's state based on QDF intensity I and its inverse I', Eqs. (35)–(38), relative to $\mathfrak{r}$, as they superpose in the direction of $\pi/3(d \to |\mathfrak{r}|)$ boxes. This is given by the input-output QDF intensity product

$$Z\Pi = Z\Pi_{|1\rangle}\pi/3 = 2\pi Z\left[9d|\mathfrak{r}\mathbf{r}|\langle\mathfrak{r}|\mathcal{T}(\mathbf{r})|\mathbf{k}\rangle\right]^{-1} = 2\pi Z\sqrt{|\langle\mathfrak{r}\mathbf{r}\rangle|}/9de^{\iota\mathbf{k}(\mathfrak{r}-\mathbf{r})}, \tag{47}$$

where there are $Z\Pi$ output states for projecting and determining a quantum state. From Eq. (42), a state prediction can be made by measuring the probability of coupling the input state and the output state. One of the output states is the final state of a box in the matrix. The matrix element between the final and initial states is $|\Delta\kappa^2\ell|$, which couples the states on a magnitude of $2|\mathbf{r}| \leftrightarrow \{|\mathfrak{r}|, 2|\mathfrak{r}|\} = |\langle\mathfrak{r}\mathbf{r}\rangle|^{1/2} \in [1, \sqrt{2}]$ positions relative to μ_{ij}, Eqs. (25)–(27). The least uncertainty expected in Eq. (25), returns $2|\mathbf{r}| \leftrightarrow |\mathfrak{r}|$ for Bob to predict. The probability density of the final energy states denotes the number of ways an ST can occur, which is determined by measuring $Z\Pi\ell$ via Eq. (46). This includes the fmv via projection products $\mathbf{P}_{\Psi\Phi}$ and $\mathbf{P}_{\Phi\Psi}$ from Eqs. (21)–(34), which obtains the quantum information about $\mathfrak{r}$.

From Eq. (10), the maximum number of particles interacting with Bob over a distance of $(2/3)d$ is

$$N_d = \max n_d. \tag{48}$$

Let N_d^2 be the area of particle interactions with Bob, where μ_{ij} from Eq. (12) is counted. The projection product $\mathbf{P}_{\Psi\Phi}$ transforms $|\phi_{i_n}\rangle$ of Φ^2 into $|\psi_{ij}\rangle$ of Ψ^2 in area N_d^2, Eqs. (21)–(29). As $d \to 1$ in Fig. 5 for $Z^{2d/3}$, the inputs relative to the projected product, return $\mathcal{P}(\Phi \to \Psi)$ from Eq. (46). This is measured by the fmv decomposed as

$$\overbrace{\lim_{d\to 1}\frac{Z}{f(N)|\Delta\kappa^2\ell|}}^{\text{fmv}} = \left|\frac{\overbrace{\Phi^2\,|\psi_{ij}\rangle\langle\psi_{ij}|N_d^2|\phi_{i_n}\rangle}^{\mathbf{P}_{\Psi\Phi}}\ln\sqrt{Z^{2/3}}}{\ell\left(\mathbf{P}_{\Phi\Psi} + Z\Pi\delta^{-1}\right)}\right|, \tag{49}$$

where the natural log ln is used to measure the ST probability from the input state coupled with the output state. Each coupled state product is measured relative to $\mathbf{P}_{\Psi\Phi}$ for any two rows of the matrix in Eq. (44). This is expressed as the sum of the products $\ell\mathbf{P}_{\Phi\Psi}$ and $\ell Z\Pi$, projected onto $\ell \in \mathbb{F}$, i.e., STs occurring between two particle sites. One site has the prize, and the other is occupied by a participant. The expected value of the quantum projector in superposition, $|\psi_{ij}\rangle$, after a Φ-field transform for all N_d, is the ST probability

$$\mathcal{P}(\Phi \to \Psi) = \left|\frac{\langle\phi_{i_n}|e^{\iota\mathbf{k}(\mathfrak{r}-2\mathbf{r})}|\psi_{ij}\rangle\langle\psi_{ij}|N_d^2|\phi_{i_n}\rangle\ln\sqrt{Z^{2/3}}}{\langle\psi_{ij}|\phi_{i_n}\rangle\langle\phi_{i_n}|\mathcal{O}^2|\psi_{ij}\rangle + \ell Z\Pi\delta^{-1}}\right| = \left|\frac{e^{\iota\mathbf{k}(\mathfrak{r}-2\mathbf{r})}N_d^2}{\delta^{-1/2}\mathcal{O}^2}\frac{|\langle\phi_{i_n}|\psi_{ij}\rangle|^2\ln\sqrt{Z^{2/3}}}{|\langle\psi_{ij}|\phi_{i_n}\rangle|^2 + \ell Z\Pi\delta^{-1}}\right|, \tag{50}$$

where projectors express the measurement of a succeeding probability value. As provided in Sec. 5.3, the information on Bob's decision is collected by a photoprobe (Alice or Eve). This occurs at a distance relative to Bob's position $\mathbf{r}$ where he makes a decision (a PT or a switch), $|\mathbf{r}| \to \lambda_{\mathrm{P}}$.

From Eqs. (27)–(34), the scattering amplitude in Eq. (50) is approximated to $f(\theta) = e^{\iota\mathbf{k}(\mathfrak{r}-2\mathbf{r})}e^{\iota\mathbf{k}(\mathfrak{r}-\mathbf{r})} = e^{\iota\mathbf{k}(2\mathfrak{r}-3\mathbf{r})} \approx 1$, where $\lambda_{\mathrm{c}} = 2|\mathbf{r}|\kappa^2/|\mathbf{r}| \to \infty$ for $\mathbf{k}_{i,j}|\mathbf{r}| = \lambda_{\mathrm{c}}^{-1}|\kappa^2| \approx 0$. This denotes that a field switch event has occurred, i.e., any 0 in matrix A, B or AB. For an energy input of N participants, a continuous transformation $\mathbf{k}_{i,j}|\mathbf{r}| \to |\mathbf{k}\mathbf{r}| \to 1$ returns a constant, Eqs. (18)–(22), by which $f(\theta) = e^{-\iota N\pi\mathbf{k}\mathbf{r}} \approx \pm 1$ is projected as an element in A or B.

From Eqs. (12), (22) and (50), as the number of pairwise particle interactions is μ_{ij}, $\mathcal{O}^2\delta^{-1/2}$ can be replaced with $\mu_{ij}/3$ from the projected product $\ell\mathbf{P}_{\Phi\Psi}$. Thus,

$$\mathcal{P}(\Phi\rightarrow\Psi)=\left|4\pi f(\theta)N_d^2\ln\sqrt{Z^{2/3}}\left[\frac{4\pi\ell\mu_{ij}}{3\delta}+\frac{\ell Z\Pi}{\delta}\right]^{-1}\right|=\left|\frac{16\pi f(\theta)(N-1)^2\ln Z^{1/3}}{9(2\pi/3\delta)\left(N(N-1)+Z/3\right)}\right|, \tag{51}$$

where the prize position $\mathfrak{r}$, depends on the sum of revolutions of a unit circle (frequency) based on the observable of each interacting particle pair, Eqs. (35)–(38). This position can be derived from $e^{i\mathbf{k}(\mathfrak{r}-\mathbf{r})}$ in the area of interaction between Bob, Alice and/or Eve, substituting the ket $|\phi_{i_n}\rangle$ of Φ, and bra $|\psi_{ij}\rangle$ of Ψ products. This denotes two particle frequencies and wavelengths from $\mathbf{k}_{i,j}^2\geq 1/4\mathbf{r}_{i,j}^2$ in Eq. (5), are separated from $\Delta\mathbf{r}_{i,j}^2$ in Eq. (22), as observed during an energy exchange via δ. From Fig. 2, each substitution of a physical variable for another is dependent on $\mathfrak{r}$, which is determined to exist in one of the two remaining boxes as the prize's quantum state teleports between them via δ.

Example 9. A quantum separation squared between four pairwise particles is $\delta^{-1}\in\mathcal{O}^4$ from Eq. (22), and satisfies any photoprobe momenta change within the range of $.5\leq\delta\lesssim 1$. For instance, Bob's state separation from a prize state via Eve who shares information about $\mathfrak{r}$ through momentum transfer, Eqs. (3)–(24). The greater the quantum separation based on δ, the greater the classical prediction in knowing which box has the prize, as a TS. *Thus, entanglement and correlation can be determined, as $N_d\rightarrow\infty$ in a QPT, and $N-1$ participants share information with Bob about the boxes. The more information $N-1$ participants share, the higher the probability of predicting the box with the prize.*

In Example 9, all participant information shared with Bob needs to be correlated to $\mathfrak{r}$. This is obtained by superposition or entanglement determined by two solutions:

1st Solution– Approximate the fmv values in Eq. (51), as $\delta\rightarrow 1$ for a strong prediction of $\mathfrak{r}$. This is based on the quantum information shared among the N participants. For a small $N>3$, and max $Z=3$, Eq. (51) is simplified to

$$\mathcal{P}(\Phi\rightarrow\Psi)=\left|f(\theta)\frac{4(N-1)^2\ln 3^{1/3}}{3(N^2-N+1)}\right|\in\left[\frac{1}{3},\frac{8\ln 3}{13}\right). \tag{52}$$

The resulting interval covers two measurement outcomes projected from their corresponding QDF circuit outputs:

1. The output is based on the information given (input) prior to a QDF transformation (at the pre-switch).
2. The output is the quantum information (qubits) exchanged at the QDF transform moment (at the switch), Sec. 4, which is based on particle superposition and entanglement, Figs. 3–5.

Example 10. From the QDF transform moment, we get the irreducible value $(8\ln 3)/13$, which satisfies an ST probability of $\mathcal{P}(\Phi\rightarrow\Psi)\approx 2/3$ on all decision cases for which box to choose, or switch to by Bob. Bob can make a prediction to win the prize as his TS based on $\mathcal{P}(\Phi\rightarrow\Psi)\approx 1/3$, given $\delta=.5$ from Eqs. (22)–(25), doubling to $2/3$, as $\delta\rightarrow 1$. This denotes a quantum separation between two interacting particles based on correlation $\langle\mathbf{kr}\rangle_{\mathrm{c}}$, from Eq. (40).

This solution cannot go above any value of the irreducible for an ST probability $>2/3$, despite having δ tending to 1. For a big N ($N\rightarrow\infty$), however, the ST probability tends to 1, which is the second solution.

2nd Solution– The ST probability reaches an irreducible based on $|\Delta\kappa^2\ell|$, which couples the input state with the output state, Eqs. (42) and (46). This can be obtained under the quantum separation condition $\delta\rightarrow 1$, as $d\rightarrow 1$ for a strong prediction, reaching ST probability values $>2/3$. This is by approximating any ST probability to an outcome based on particle entanglement, which assures a classical prediction (zero superposition) of $\mathfrak{r}$ as

$$\mathcal{P}(\Phi\rightarrow\Psi)\approx 4(N-1)^2/9\vartheta_{ij}\mu_{ij}\geq 2/3, \tag{53}$$

where $8/9\leq\vartheta_{ij}\leq 1$ is the pairwise particle adjustment factor, adjusting the result against the irreducible $8/9$ produced for a big $N\gg 3$. The adjustment ϑ_{ij} is applied due to one particle of the pair *misbehaves* (uncontrolled) within the

given range. The prize in this range is superposing with a level of uncertainty ≈ 0.1 or 10%, which is $\geq 90\%$ probability to be in position $\mathfrak{r}$. Thus, an ST probability of $\mathcal{P}(\Phi \rightarrow \Psi) \approx 1$, is by projecting and coupling an input state with an output state based on superposition between the participants and the prize, Secs. 2.2, 4.2, and [7]. The projection and coupling satisfy a TS attainable by a pair of one or more participants who expect Alice's or Bob's TS.

From Eq. (46), we can examine different ST probability values for $Z \in [1,3]$ via $f(\kappa)$ and $N > 3$ between the input and output sides of ρ_{AB} in Eq. (44). The results vary between 0 and .9, depending on δ from Eqs. (50)–(53). Based on $\min \mathcal{P}(\Phi \rightarrow \Psi) = 1/3$, the results can be shown in a QDF density matrix

$$|\rho_{AB}| = \frac{AB^{|\cdot|} \rightarrow B^{|\cdot|}}{f(N)|\Delta\kappa^2 \ell|} = \left\{ \frac{\mathcal{P}(\Phi \rightarrow \Psi)AB^{|\cdot|}}{3} \longrightarrow \textcircled{\scriptsize S} \longrightarrow \frac{\mathcal{P}(\Phi \rightarrow \Psi)B^{|\cdot|}}{\{1,2\}} \right\} = \overbrace{\begin{bmatrix} .4 & .0 & .6 \\ .6 & .4 \leftrightarrow .0 & .0 \leftrightarrow .3 \\ .2 & .5 \leftrightarrow .2 & .3 \leftrightarrow .6 \end{bmatrix}}^{\frac{\mathcal{P}(\Phi\rightarrow\Psi)AB^{|\cdot|}}{3} \rightarrow \textcircled{\scriptsize S} \rightarrow \frac{\mathcal{P}(\Phi\rightarrow\Psi)B^{|\cdot|}}{\{1,2\}}}, \tag{54}$$

where the absolute values of the matrix elements, denoted by $|\cdot|$, consist of the results obtained from Eqs. (44)–(46) and (53). For each *transition step* [96], an ST occurs from the left, the input, to the right, the output. The left matrix elements denote participant inputs from AB, and those in the middle column denote the field switch event Ⓢ from A. Each of the right elements denotes the state of a box according to B. The sum of ST probabilities in each row is 1.

Example 11. One of the two right matrix elements has a probability of .6 that a box for Bob is in state $|2\rangle$ to choose (steps 5–7). A probability of .3 exists as the remaining element for the box to have the prize. The switch values in the middle column are set to 0 when Bob decides at model step 7. A probability > 0 at the switch, means the system will remain in the ES or GS, as Bob assumes $|i_n\rangle$ about $\mathfrak{r}$, $\mathfrak{r}$ correlates with $\mathbf{k}$ of a photon projecting onto $\mathcal{S}_{\mathfrak{r}}$ by Alice. This occurs between the switch and the output on the basis of $|0\rangle$ and $|1\rangle$ in their corresponding rows. At the switch, a probability of .4 denotes Bob to stay undecided (step 5). This is assuming that there have been two inputs. One input is with probability .4 (top left element), resulting in a probability .6 as a box with the prize. This state occurs via the *nonzero switch state* in the middle column, returning an ES $\leftrightarrow$ GS in the right column. This is when from the middle row output, .3 doubles to .6 via $|12\rangle$, or $|1\rangle$ and $|2\rangle$ in the top row, as opposed to the bottom row's output state $|02\rangle$, Fig. 4. The other input (middle left element) is with probability .6 resulting in a probability .3 as prize state $|1\rangle$ (middle right element). Bob's decision for $i = 1$ from quantum state $|12\rangle$ versus $|02\rangle$ can output $i = 0$ in the bottom row, see Eq. (9) for Table 1. This classical state about $\mathfrak{r}$ can be extracted from a quantum state based on $|\kappa^2|\varrho \leq 2$, Eqs. (41)–(54). This is if the norm $\|AB\|^{1/2} \leq 2$ contains the quantum information on $\mathbf{k}\mathfrak{r}$ as the product of a photonic and atomic interaction between Bob, a participant, and the prize. Thus, an ES $|1\rangle$ denoting $\mathfrak{r}$ can be predicted by extracting the classical state $i = 1$ from entanglement between Bob and the prize, $|11\rangle$ (see [28]).

■

Remark 13. From $\|AB\|^{1/2}$, $\|AB\| \leq \|AB\|_\infty = 4$ is the infinity norm denoting the geometry of particle state projections between four field positions in Eq. (27). A mixed state is when the trace $\mathrm{tr}|\rho_{AB}^2| < 1$, since $\|AB\|_\infty > \|AB\|^{1/2}$. A separable state is when $\mathrm{tr}|\rho_{AB}^2| = 1$ as $d \rightarrow 0$ in Δd, Eq. (31), relative to the change in the matrix norm $\|\Delta AB\| = |\mathrm{tr}\, B - \mathrm{tr}\, A| = 1$. This change denotes a field switch event Ⓢ between 0 and a nonzero switch state. Entanglement can be extracted from the Bell states between A and B.

Remark 14. One of the matrix two bottom rows in Eq. (54) denote a poor imitation of the prize or no prize (a PNS attack) at $|\mathfrak{r}| \rightarrow 2|\mathbf{r}|$, which corresponds to Fig. 4 events. Quantum entanglement between Bob at $\mathbf{r}$ and the no prize state, relative to the opposite state at $\mathfrak{r}$ as his TS, can be determined from the matrix bottom row values.

In summary, the proof of the theory presents the statistical significance of a QDF transformation in predicting events within the probabilistic and determinist pictures of the model, Sec. 2.2. The proof also provides a prediction of an output state and a TS at the PT level based on a field switch, Eq. (16). The switch conducting e.g., an $\oplus$ or $\otimes$ operation for a QDF transformation, is implemented in a QDF circuit [7]. The circuit's output, given the ST probability from Eq. (53), is validated by correlating the ST probability results of a measurement made on entangled qubit pairs,

with their decoded classical bits [7], Examples 2 and 3. This observation is based on the input-output state coupling of a particle via projection (PDI from a specific party as listed in Table 1) and particle pairing, Sec. 6.3.

8. QDF information for Bob

At model step 3 of Fig. 1 or 6, between the three boxes, Bob has a probability of .3 to be in a GS or ES. At step 4, after Bob chooses a box, e.g., state $|1\rangle$, under the κ-based field transformation in Eq. (39), Alice reveals a box with no prize $i = 0$, from one of the two remaining boxes with prize state $|0_m\rangle$, relative to Bob's initial choice as $|1\rangle$.

At step 5, Bob's assumption about the prize position $\mathfrak{r}$ is $\geq .6$ if he chooses the remaining box as $|2\rangle$ between his initial choice and the one he just made, thus producing a mixed state of 0 and 1. This can result in state $|0\rangle$ at step 6. From Eqs. (10) and (41), the following density matrix shows which box is with and without a prize, according to Bob:

$$|\rho_B| = |\psi_{i_n}\rangle\langle\psi_{i_n}|/\left|\Delta\kappa^2\ell\right| = \mathcal{P}'|1\rangle\langle 1| + \mathcal{P}|2\rangle\langle 2|, \tag{55}$$

where $\mathcal{P}' = 1 - \mathcal{P}$ is the ST probability of the complement of no prize or a/the prize to exist in a box, i.e., $\mathcal{P}(\Phi \to \Psi)$ from Eq. (53), and $|\rho_B|$ is a submatrix of $|\rho_{AB}|$ in Eq. (54), [95]. Bob can have his state entangled with state $|1\rangle$, Eq. (39), and increase his chance of winning to $.6|2 \to 1\rangle = .6|1\rangle$ by accessing the quantum information from Eq. (54). Bob can adapt to a quantum measurement setup by Alice over the three boxes to make a decision (switch?). If like Alice, Eve in superposition $2\ell r$, Eq. (20), reads and shares information about $\mathfrak{r}$ with Bob, as $\langle 2\ell r\rangle = 2|\mathbf{r}| \leftrightarrow |\mathfrak{r}| = |\langle \mathfrak{r}\mathbf{r}\rangle|^{1/2} \to 1$, Eqs. (25)–(31), then with the least uncertainty expected in Eq. (25), Bob has a chance to win the prize as his TS.

For $N - 1$ participants interacting with Bob, as their positions and momenta correlate based on Eqs. (22)–(41), superposition becomes entanglement between Bob and the prize [26], which gives Bob a probability close to 1 in predicting $\mathfrak{r}$ from Eq. (53). This prediction of classical state i, is obtained from the expected position $|\langle \mathfrak{r}\mathbf{r}\rangle|^{1/2} \to 1$ in Fig. 3(c), which is zero superposition. This relates to predicting states from entangled EPR pairs in Sec. 4.2.2.

9. Conclusion and future work

A phase transition (PT) was characterized and predicted in a quantum double-field (QDF) model using correlation and scalar functions, $\langle\Psi\Phi\rangle$ and $f(\kappa)$, respectively. Quantum measurement and scalar readout points were introduced to satisfy these functions in defining system measurement outcomes between their probabilistic and deterministic pictures. For this, a projective decomposition of identity (PDI) of outcomes was introduced and chosen to solve measurement problems. This required the use of scalar κ and particle pairing to obtain two compatible measurements relative to incompatible observables in the system. A state transition probability was calculated to describe these measurements on a particle state from a QDF transformation in a transition density matrix. The matrix values denote a field switch state and a particle state. From these values, entanglement and separable states for detecting a prize state were determined on a spatial magnitude of $|\kappa^2|\varrho \leq 2$, doubling the probability of a prize win or loss (a PT) with a $\mathcal{P} \geq 2/3$ in the QDF.

Bob in the game, as a particle, obtains the QDF information from an invisible third party, Eve, who observes Alice and the boxes. Alice however, sets up the prize as a quantum particle to superpose among the boxes as her target state (TS). If Bob correlates the prize position $\mathfrak{r}$, with what he assumed first to be the box having the prize from his position $\mathbf{r}$, he wins the prize as his TS, against Alice's TS, whereas the latter assures Bob to win no prize or only a prize, not the prize. The question remains, can his assumed state entangle with the final state of the box having the prize? This is done by mapping the correlation length λ_c to $|\kappa^2|$ bounds associated to his field, paired with the prize and Alice's superposition field, transforming his classical field to a quantum field as an entangled particle. This can be shown as entangled EPR pairs produced in a quantum experiment. For example, photonic probes such as Eve intercept information on the prize while being superposed by Alice. This information is encoded in qubits, where qubit teleportation between boxes is observed through Bell state measurements in a QDF circuit. This circuit was presented based on the PDI of outcomes, given an input state from the field Ψ or Φ, followed by $f(\kappa)$ satisfying a field switch to project the system measurement outcome.

The metric geometry for particle state projections on the $|\kappa^2|^{\pm 2}$ bounds within the κ-limit, showed the prize for Bob, and Alice's interaction distance close to, and far from the Planck length λ_P. For a box with a prize or no prize state, Bob must obtain a distance of $d = \lambda_c^{-1}|\kappa^4| \gtrsim \lambda_P$, observing QPTs via entanglement as an entangled EPR pair. Consequently, Bob wins the prize at $d = \lambda_c|\langle \mathfrak{r}\mathbf{r}\rangle/\kappa^4| \gg \lambda_P$. The distance between Bob and the prize is $d \to 1$, and from his area of particle interactions $d^2 \to r\lambda_P$, he predicts the prize from its QDF. The information from a QDF at

distance $d \leq 1$ within the open-closed areas of singularity, is based on the particle's input state, coupled or entangled with its output state according to Fermi's golden rule. This rule satisfies any qubit measurement in the QDF circuit to determine and predict particle states within e.g., heat engines, condensed matter, and game theory models.

A QDF lens coding method [7], from the model, is proposed to implement a QDF circuit on a quantum computer. The QDF circuit performs the QDF transform and its compatibility to quantum Fourier transform on qubits. The QDF of the circuit's input and output, constructs an efficient heat engine which is evaluated based on the measurement of qubits from the QDF. From the measurement data, entanglement and PTs are predicted, showing how the QDF can be used to make strong predictions of the next system state as it evolves over time. Its simulation review [8], compares the model to current quantum simulators, and concludes QDF to consistently give strong system state predictions.

Acknowledgments

P. B. A. acknowledges Dr. W. Chen endorsement from the Institute of Theoretical Physics at ETH Zürich, for comments on condensed matter physics. P. B. A. also acknowledges the University of Victoria Canada, for financial support. P. B. A. and T. A. G. thank Dr. T. Lu for his comments on the scalar field physics, Dr. M. Laca for his comments on the fmv (four measurement variables) equations, Eqs. (12)–(53), and the late Dr. F. Diacu for his input on quantum phase transitions and probability bounds in the proposed model.

Appendix A A QDF game

The following is an adaptation of the system model steps presented in Sec. 1 and Fig. 1, as a QDF game, which projects events and their measurement outcome to a double-field metric space [2–4]. The QDF game does not dictate the quantum physics of particles interacting and communicating in any experiment. This game rather examines the theoretical and experimental aspects of STs, such as energy exchanges on QPT and CPT scales for any thermodynamic system discussed in [7] results, analysis and conclusions.

In this game, the thermodynamic model is introduced based on a game with N interacting participants, as defined in Sec. 1 QDF model. There are two versions of this game. One version is the classical Monty Hall problem [13–15], and the other is the proposed quantum model. The participants are Alice the host, Bob the guest, Eve who observes the interactions between Bob and Alice, and $N - 3$ audience members. There are three boxes and a prize to win. The steps of the game as animated in Fig. 6 are as follows.

1. A prize is hidden by Alice in one of the three boxes. *In the classical model, she cannot change its position as* $\mathfrak{r}$*, until a new game. In the proposed quantum model, she can change its position with a magnitude of* $|\mathfrak{r}| < \infty$.
2. Alice knows where the prize is, while Bob does not.
3. Bob is asked to choose one of the three boxes.
4. Alice opens another box to show there is no prize in it (1/3 of all information or binary message).
5. Bob can remain with his initial choice or switch to the other remaining box (a binary choice).
6. The participants can suggest a box for Bob to choose. Eve, as an invisible observer, with a given probability gathers information by looking inside each box. Eve with some probability shares her information with Bob about the contents of each box. *In the quantum model, as Alice changes the prize position, Eve intercepts any state transfer between boxes based on a quantum state teleportation, e.g., see step 6 in Sec. 1.*
7. Bob chooses a box and either wins the prize or a prize with a cheaper value as a *poor imitation* of it (a bad copy as some of the prize energy), or loses.

In this model, the collective energy input and output determine Bob's decision outcome as no prize, a prize or the prize in this game. As shown in Fig. 6, the audience colored in yellow, guess and suggest according to Alice's suggestion to Bob in step 6, whereas their total energy is one of the inputs to Bob. The audience colored in gray remain uncertain and can go with either Bob or Alice (Eve is invisible to them) as another energy input. The audience colored in black favour what Bob chooses and decides between steps 5–7 as the final energy input.

The energy output represents the game outcome which determines Bob's win of a/the prize against Alice. Bob is either excited with the audience or grounded due to a no prize win compared to Alice who is excited as the winner against Bob. If Bob is the loser, then all participants prepare to input their total energy for the next round of the game.

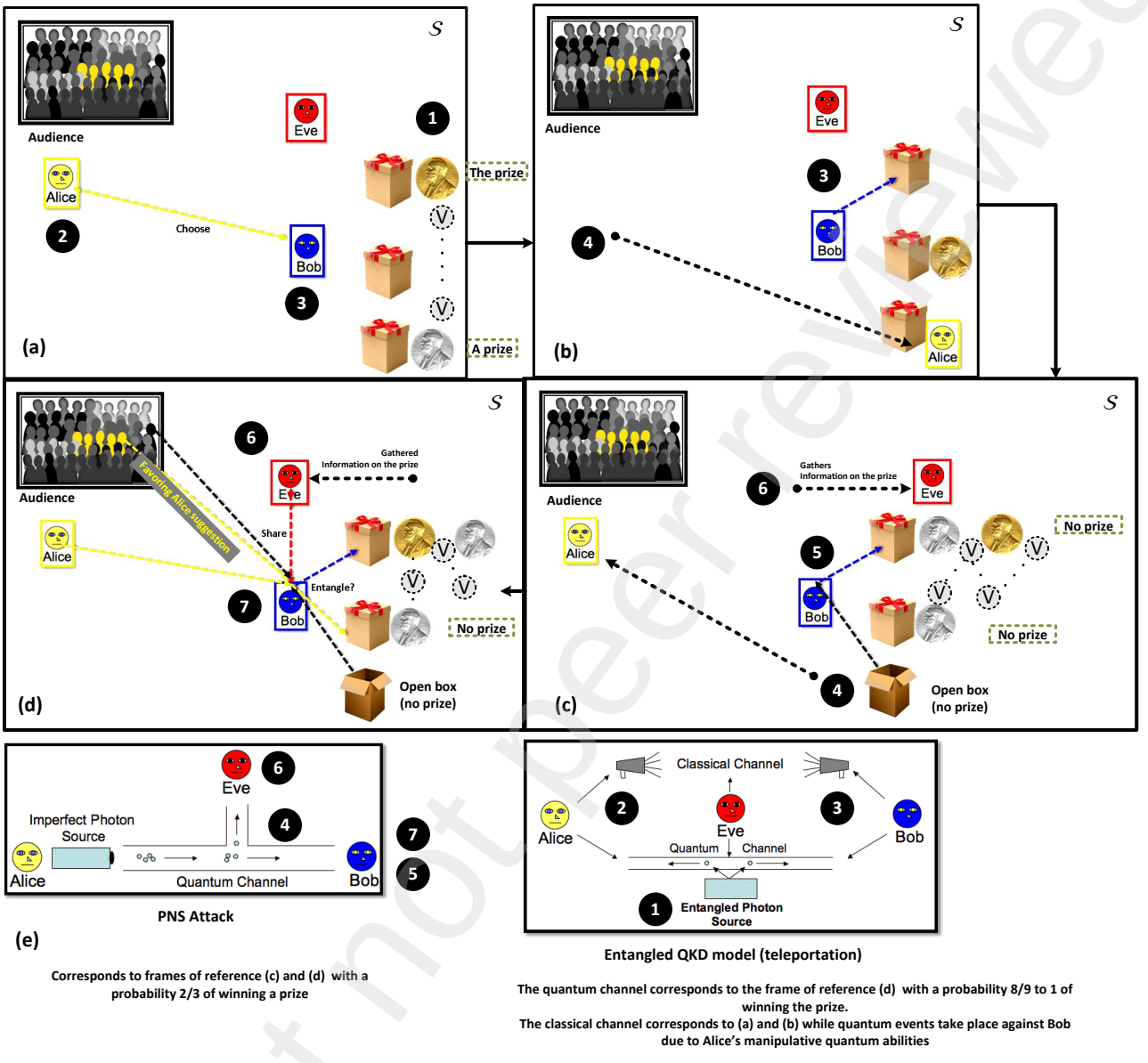

Fig. 6: **(a)-(d)** QDF game theory model animation (see Appx. B or [9] to run this) with participants presented with their energy exchange between game steps 1–7 to share, guess, hide or gather information on the prize position $\mathfrak{r}$. The game thermodynamics can be mapped from the game steps played by the participants as particles interacting in the game. A participant inputs energy (suggestion/decision), and interacts with another participant resulting in an energy output in game space $\mathcal{S}$. A classical or quantum measurement can be done on this space [73], and Bob is in this space an atom exchanging energy with others. **(e)** Left image corresponds to the animated reference frames **(c)** and **(d)** with a probability 2/3 for Bob winning a prize. Right image, the quantum channel corresponds to the frame of reference **(d)** (or in Fig. 1**(b)**) with a probability 8/9 to 1 of winning the prize (to validate, see Sec. 7 proof, or Eq. (53)). The classical channel corresponds to **(a)** and **(b)** while quantum events take place against Bob due to Alice's manipulative quantum abilities. For example, the creation of EPR pairs is followed by a QKD versus a PNS attack, Sec. 2.2. (Images in **(e)**, courtesy of Haitjema [32] and [33].)

The experimental evaluation of both, the particle interaction aspects in the QDF model and this game is presented through examples available from [7, 9]. The method paper represents the methodical approach to satisfy two experimental objectives, achieving a thermodynamic system measurement goal, as well as the presentation of the theoretical

concept of the QDF model and this game using qubit processing techniques on quantum machines. The results in the method paper are presented according to the standards known in quantum mechanics and thermodynamics.

Appendix B Supplementary documents

Online mathematical tools [97] were used to conduct computations to validate the QDF model and evaluate the fmv equations. In addition, the method paper [7] implements and further validates the QDF model proving its universality for a set of CPTs and QPTs observed in a thermodynamic system. Lastly, the QDF game demo and relevant data are available in the Supplementary Information file, or [9].

References

[1] G. Ekspong (ed.), Nobel Lectures, Physics (1996-2000), *Nobel Lecture by William D. Phillips, Dec. 8, 1997,* (WSP, Singapore, 2002), 199–237.
[2] S. Rastgoo, M. Requardt, Emergent space-time via a geometric renormalization method, Phys. Rev. D 94 (12) (2016) 124019.
[3] M. Damian, S. Pandit, S. Pemmaraju, Distributed Spanner Construction in Doubling Metric Spaces in: Principles of Distributed Systems (Springer, 2006) LNCS 4305, pp. 157–171. Full conference series paper available at ResearchGate in 2015.
[4] D. Eppstein, H. Khodabandeh, Distributed construction of lightweight spanners for unit ball graphs in: 34th ACM Symposium on Parallelism in Algorithms and Architectures, 2022, pp. 57–59. Full article preprint available at arXiv:2106.15234 (2021).
[5] H. Bluhm, T. Calarco, D. DiVincenzo (Eds.), *Quantum Technology: Lecture Notes* at IFF Spring School 2020, 20 (2020), Chaps. A2–A5, B4.
[6] N. Sultana, *Single-photon detectors for satellite based quantum communications* (Ph.D. Thesis, Waterloo Univ., 2020) Chap. 8.
[7] P. B. Alipour, T. A. Gulliver, Quantum Field Lens Coding and Classification Algorithm to Predict Measurement Outcomes, MethodsX, Elsevier BV (2023) 102136, doi:10.1016/j.mex.2023.102136.
[8] P. B. Alipour, T. A. Gulliver, Quantum AI and Hybrid Simulators for a Universal Quantum Field Computation Model, *to appear on* MethodsX, Elsevier, MEX-D-23-00171(2023).
[9] P. B. Alipour, T. A. Gulliver, QF-LCA dataset: Quantum Field Lens Coding Algorithm for system state simulation and strong predictions, *to appear on* Data in Brief, Elsevier BV (2023). Source code available on Mendeley Data, Elsevier BV (2022) V2^{+}, doi:10.17632/gf2s8jkdjf.
[10] A. Peres, D. R. Terno, Quantum information and relativity theory, Rev. Mod. Phys. 76 (2004) 93.
[11] P. E. Black, D. R. Kuhn, C. J. Williams, *Quantum Computing and Communication, Advances in Computers* (Elsevier, 2002) Sec. 3.4.
[12] C-R. Wie, Two Qubit Bloch Sphere, Phys. (2) 3 (2020) 383–396.
[13] J. P. Morgan, N. R. Chaganty, R. C. Dahiya, M. J. Doviak, Let's Make a Deal: The Player's Dilemma, Amer. Stat. 45 (1991) 4.
[14] A. P. Flitney, D. Abbott, Quantum version of the Monty Hall problem, Phys. Rev. A 65 (2002) 062318.
[15] G. Dariano, R. Gill, M. Keyl, R. Werner, B. Kümmerer, H. Maassen, The quantum Monty Hall problem, QIC, Rinton Press 2 (2002) 5.
[16] K. Bolonek-Laso, Three-player conflicting interest games and nonlocality, Quant. Info. Process. 16 (2017) 8.
[17] J. Marckwordt *et al.*, Entanglement Ball: Using Dodgeball to Introduce Quantum Entanglement, Phys. Teach. 59 (2021) 613.
[18] D. G. Angelakis, M. Christandl, A. Ekert, *Quantum information processing: from theory to experiment,* IOS Press 199 (2006) 109–112.
[19] J. A. Miszczak, P. Gawron, Z. Puchala, Qubit flip game on a Heisenberg spin chain, Quant. Info. Processing 11 (2012) 1571-1583.
[20] S. Khan, M. Ramzan, M. K. Khan, Decoherence Effects on Multiplayer Cooperative Quantum Games, Commun. Theor. Phys. 56 (2011) 228.
[21] G. P. Berman *et al.*, BEC of ultra-light axions as a candidate for the dark matter galaxy halos, Mod. Phys. Lett. A, WSP 34 (2019) 30.
[22] R. Casadio, A. Giugno, O. Micu, A. Orlandi, Thermal BEC black holes, Entropy 17 (2015) 10, 6893–6924.
[23] W. Unruh, Experimental black hole evaporation, Phy. Today, AIP (2016).
[24] G. Dvali, C. Gomez, Black holes as critical point of quantum phase transition, Eur. Phys. J. C, Part. Fields 74 (2014) 2 74, 2752.
[25] Cmte. on AMO 2010, *Controlling the Quantum World: The Science of Atoms, Molecules, and Photons* (NRC, USA, 2007) Chaps. 2–7.
[26] P. Ball, *Building the quantum internet* (Oxford Univ. Press, 2018), Nat. Sci. Rev. 6 (2019) 374—376.
[27] J. Higbie, D. M. S-Kurn, Generating macroscopic-quantum-superposition states in momentum and internal-state space from BECs with repulsive interactions, Phys. Rev. A 69 (2004) 053605.
[28] B. Hacker *et al.*, Deterministic creation of entangled atom–light Schrödinger-cat states, Nat. Photon. 13 (2019) 110—115.
[29] J. F. Clauser, M. A. Horne, A. Shimony, R. A. Holt,An experiment to test local hidden-variable theories, Phys. Rev. Lett. 23 (1969) 880.
[30] R. F. Werner, M. M. Wolf, Bell inequalities & entanglement, Quant. Info. Comp., Rinton Press 1 (2001) 3.
[31] M. Nielsen, I. Chuang, *Quantum Computation and Quantum Information* (Cambridge Univ. Press, UK, 2010), 25–28, 96–113, 541, Sec. 12.6.
[32] M. Haitjema, *A Survey of the Prominent Quantum Key Distribution Protocols*, available online at semanticscholar.org, WA Univ., USA (2007).
[33] L. Ma, O. Slattery, X. Tang, Optical quantum memory and its applications in quant. communications, J. Res. USA 125 (2020) 125002.
[34] M. Lopes, N. Sarwade, Cryptography from quantum mechanical viewpoint, IJCIS 4 (2014) 2.
[35] C. Macchiavello, G. M. Palma, A. Zeilinger, *Quantum Computation and Quantum Information Theory* (WSP, 2000), pp. 40–52.
[36] D. Llewellyn *et al.*, Nat. Phys. 16 (2020) 148–153; D. Nield, *chip-to-chip quantum teleportation* (Bristol Univ. UK, Dec. 2019).
[37] C. H. Bennett *et al.*, Teleporting an unknown quantum state via dual classical and EPR channels, Phys. Rev. Lett. 70 (1993) 1895.
[38] V. Khemani, C. R. Laumann, A. Chandran, Many-body localization and symmetry-protected topological order, Phys. Rev. B 99 (2019) 161101.
[39] S. Chaudhuri, S. Roy, C. S. Unnikrishnan, BEC in optical traps and in a 1D optical lattice, Current Sci. 95 8 (2008) 1026–1034.
[40] K. Kim, M-S. Chang, S. Korenblit, *et al.*, Quantum simulation of frustrated Ising spins with trapped ions, Nat. 465 (2010) 590—593.
[41] Y-L. Xu, X-M. Kong, Z-Q. Liu, C-Y. Wang, Quantum entanglement and quantum phase transition for the Ising model on a two-dimension square lattice, Physica A: Stat. Mech. 446 (2016) 217–223.
[42] U. Faigle, M. Grabish, Game theoretic interaction and decision: a quantum analysis, Games 8 (2017) 48.
[43] J. Bird, C. Ross, *Mechanical Engineering Principles* (Routledge UK, 4th ed., 2020) 42.

[44] J. Stolze, D. Suter, *Quantum Computing* (Wiley-VCH, 2004) pp. 5, 44–58, 88–95, 145–179, and Chap. 13.
[45] A. Peres, *Quantum Theory: Concepts and Methods* (Kluwer, NY USA, 2002) 373–374.
[46] X. Guo, Y. Mei, S. Du, Testing the Bell inequality on frequency-bin entangled photon pairs, Optica 4 (2017) 4.
[47] M. Hayashi, S. Ishizaka, A. Kawachi, G. Kimura, T. Ogawa, *Introduction to Quantum Information Science* (Springer, 2014) 81–85.
[48] Z. Cheng, J. H. Man, Accurate analytic solution for ideal boson gases in a two-dimensional harmonic trap, Can. J. Phys. 98 (2020) 2.
[49] B. C. Hall, *Quantum Theory for Mathematicians* (Springer, 2013) Chaps. 11 and 12.
[50] L. de la Peña, A. V-Hernández, A. Cetto, Statistical consequences of the harmonic oscillator zero-point energy, Amer. J. Phys. 76 (2008) 947.
[51] D. D'Alessandro, *Introduction to Quantum Control and Dynamics* (CRC press, NW, 2008) Chaps. 1–4, 8, 9.
[52] F. Mandl, G. Shaw, *Quantum Field Theory* (Wiley Press, 2010) pp. 2–126, and Chap. 18.
[53] J-L. Basdevant, J. Dalibard, *Quantum Mechanics* (Springer, 2007), 2nd ed., Chaps. 2, 4–6.
[54] E. Saglamyurek *et al.*, Storing short single-photon-level optical pulses in Bose–Einstein condensates, New J. Phys. 23 (2021) 043028.
[55] P. Zoller (Lorentz Chair, 2005). *Lecture Notes on Quantum Optics and Quantum Information*, at https://www.lorentz.leidenuniv.nl/lorentzchair/zoller/, Inst. for Theor. Phys., Innsbruck Univ., Austria (2005) [Accessed, 2021].
[56] Y. Jing *et al.*, Split spin-squeezed bose–einstein condensates, N. J. Phys. 21 (2019) 093038.
[57] M. Chaudhary, M. Fadel, V. Ivannikov, T. Byrnes, Teleportation protocol for split-squeezed BECs, AIP Conf. Proc. 2241 (2020) 020010.
[58] Y. Wang, Z. Hu, C. Sanders, S. Kais, Qudits and High-D Quantum Computing, Front. Phys. 8 (2020) 479.
[59] J. Pinnell, I. Nape, M. de Oliveira, N. TabeBordbar, A. Forbes, Experimental Demonstration of 11-Dimensional 10-Party Quantum Secret Sharing, Laser Photonics Rev. 14 (2020) 2000012.
[60] W. S. Martins *et al.*, Efficient atomic memory using electromagnetically induced absorption, Phys. Open 9 (2021) 100081.
[61] X-X. Yi, H-J. Wang, C-P. Sun, Bose–Einstein Condensation in Harmonic Oscillator Potentials, IoP Phys. Scr. 57 (1998) 324.
[62] M. G. Moore, P. Meystre, Generating Entangled Atom-Photon Pairs from Bose-Einstein Condensates, Phys. Rev. Lett. 85 (2000) 5026.
[63] R. Howl, R. Penrose, I. Fuentes, Exploring the unification of quantum theory and general relativity with a BEC, N. J. Phys. 21 (2019) 043047.
[64] T. K. Hakala *et al.*, Bose-Einstein condensation in a plasmonic lattice, Nat. Phys. 14 (2018) 739–744.
[65] X. He *et al.*, Carbon nanotubes as emerging quantum-light sources, Nat. Mat. 17 (2018) 663–670.
[66] F. R. G. Bagsican *et al.* Terahertz Excitonics in CNTs: Exciton Autoionization, and Multiplication Nano Lett. 20 (5) (2020) 3098–3105.
[67] P. Pessoa, C. Cafaro, Information geometry for Fermi–Dirac and Bose–Einstein quantum statistics, Physica A, 576 (2021) 126061.
[68] P. Gawron, Noisy quantum Monty Hall game, Fluct. Noise Lett. 9 (2010) 1.
[69] P. Frąckiewicz, A. G. M. Schmidt, N-person quantum Russian roulette, Physica A 401 (2014) 8-–14.
[70] A. Borzi, G. Ciaramella, M. Sprengel, *Formulation and Numerical Solution of Quantum Control Problems* (SIAM, USA 2017), Chaps. 2.6–2.8.
[71] W-M. Liu, Emmanuel Kengne, *Schrödinger Equations in Nonlinear Systems* (Springer, 2019) Chaps. 1.3, 10.5 and 10.6.3.
[72] L. Asteria *et al.* Quantum gas magnifier for sub-lattice-resolved imaging of 3D quantum systems, Nat. 599 (2021) 571—575.
[73] R. B. Griffiths, Quantum measurements and contextuality, Phil. Trans. R. Soc. A 377 (2019).
[74] R. B. Griffiths, What Quantum Measurements Measure, Phys. Rev. A 96 (2017) 032110; *Quantum Measurements and Contextuality*, C-Mellon Univ. USA (2018); *Consistent Quantum Theory* (Cambridge Univ. Press, 2003), Chaps. 1, 2.2, 4.6, 18.4, 22.5.
[75] S. Abramsky, R. S. Barbosa, S. Mansfield, Contextual Fraction as a Measure of Contextuality, Phys. Rev. Lett. 119 (2017) 050504.
[76] G. A-Camelia, S. Majid, Waves on Noncommutative Spacetime and Gamma-Ray Bursts, J. of Modern Phys. A 15 (2000) 4301–4323.
[77] E. Castellanos, T. Matos, Klein Gordon Fields and Bose-Einstein Condensate, Int. J. Mod. Phys. B 27 (2013) 1350060.
[78] L. D. Carr, *Understanding Quantum Phase Transitions* (CRC Press, USA, 2010) Sections 1.2, 1.6, 2.0, 2.1, 2.3, 3.
[79] T. Vojta, Phases and phase transitions in disordered quantum systems, AIP Conf. Proc. 1550 (2013) 188.
[80] C. V. Vliet, *Equilibrium and Nonequilibrium Statistical Thermodynamics* (WSP, 2010) pp. 5–42, 95–163, 201–291, 339–400, 540–542, 811.
[81] C. A. Regal, M. Greiner, D. S. Jin, Observation of Resonance Condensation of Fermionic Atom Pairs, Phys. Rev. Lett. 92 (2004) 040403.
[82] O. M-Aldama, Spontaneous Symmetry Breaking in Hyperbolic Field Theory, IoP J. Phys. Conf. Ser. 761 (2016) 012048.
[83] M-J. Hwang, R. Puebla, M. B. Plenio, Quantum phase transition and universal dynamics in the Rabi model, Phys. Rev. A 94 (2016) 023835.
[84] M. G. Vasin, V. Ryzhov, V. M. Vinokur, Quantum-to-classical crossover near quantum critical point, Sci. Rep. 5 (2015) 18600.
[85] M. G. Vasin, V. M. Vinokur, Bose system critical dynamics near quantum phase transition, Physica A 575 (2021) 126035.
[86] D. McMahon, Quant. Mech., *Quantum Mechanics Demystified* (McGraw Hill, NY, USA, 2013) Chaps. 8–11.
[87] B. Scott, *Elements of Quantum Optics* (Edtech Press, UK, 2019) Chaps. 2 and 3.
[88] D. Wang, F. Ming, M-L. Hu, L. Ye, Quantum-Memory-Assisted Entropic Uncertainty Relations, Ann. Phys. (Berlin) 531 (2019) 1900124.
[89] H. Zhu, Zero uncertainty states in the presence of quantum memory, Quant. Info., NPJ 7 (2021) 47.
[90] S. Xu, J. Schmiedmayer, B. C. Sanders, Nonlinear quantum gates for a Bose-Einstein condensate, Quant. Phys. arXiv:2201.02964 (2022).
[91] J. S. Briggs, A derivation of the time-energy uncertainty relation, IoP J. of Phys., Conf. Series 99 (2008) 012002.
[92] R. Fitzpatrick, *Position, Momentum*, and *Heisenberg's Uncertainty Principle* (Sci. Press, 2015) Chap. 2.
[93] N. Zettili, *Quantum Mechanics: Concepts and Applications* (Wiley Press, 2nd ed., 2010) 623–628, 637–639.
[94] T. D. Bradley, (Ph.D. in Math. and Qaunt. Theo.), *What is applied category theory?* (2020) Quant. Phys. arXiv:2004.05631. Pages 9–11, 22, 43–50, NY Univ., USA; *Tensor Product on Qunatum Particles* (2020).
[95] C. M. Alves, *Detection of quantum entanglement in physical systems* (Ph.D. Thesis, Oxford Univ., 2005) Chap. 2.
[96] D. A. Kofte, *Lecture Notes on Transition Probability Matricies*, *Molecular Simulation*, at http://www.eng.buffalo.edu/~kofke/ce530/Lectures/Lecture8/index.htm, Buffalo Univ., USA (2000) [Accessed, 2016].
[97] S. Wolfram, *Mathematica Computational Systems* at: wolframalpha.com; Microsoft's Azure Quantum at: http://docs.microsoft. com/en-us/quantum [Accessed, 2015–2021].